Hydrogen-bonded water-wires/clusters -toward natural selectivity of artificial water channels

Dan-Dan Su, Mihail Barboiu

▶ **To cite this version:**

Dan-Dan Su, Mihail Barboiu. Hydrogen-bonded water-wires/clusters -toward natural selectivity of artificial water channels. Coordination Chemistry Reviews, 2024, 515, pp.215973. 10.1016/j.aebj.2014.10.012 . hal-04742128

HAL Id: hal-04742128
https://hal.science/hal-04742128v1

Submitted on 17 Oct 2024

HAL is a multi-disciplinary open access archive for the deposit and dissemination of scientific research documents, whether they are published or not. The documents may come from teaching and research institutions in France or abroad, or from public or private research centers.

L'archive ouverte pluridisciplinaire **HAL**, est destinée au dépôt et à la diffusion de documents scientifiques de niveau recherche, publiés ou non, émanant des établissements d'enseignement et de recherche français ou étrangers, des laboratoires publics ou privés.

Available online at www.sciencedirect.com

Coordination Chemistry Reviews

journal homepage: www. elsevier.com/locate/ccr

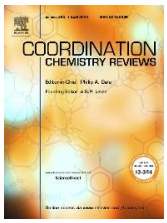

Review

Hydrogen-bonded water-wires/clusters -toward natural selectivity of artificial water channels

***Dan-Dan Su*[a], *Mihail Barboiu*[a,b]*

[a] *Institut Européen des Membranes, Adaptive Supramolecular Nanosystems Group, University of Montpellier, ENSCM-CNRS, Place E. Bataillon CC047, Montpellier, F-34095, France.*

[b] *Babes-Bolyai University, Supramolecular Organic and Organometallic Chemistry Center (SOOMCC), Cluj-Napoca, 11 Arany Janos str., RO-400028, Cluj-Napoca, Romania.*

ARTICLE INFO

Article history:
Received 00 December 00
Received in revised form 00 January 00
Accepted 00 February 00

Keywords:
Natural porins
Artificial water channel
Hydrogen bonding
Water wires

ABSTRACT

Efforts toward the denovo design of artificial water channels have been made over the last decades to understand the selectivity of water transport through membranes and their applications in water purification and desalination. Currently, many insights are needed to elucidate the complex selective water *vs* ion/proton transport mechanism through Å-scaled artificial water channels. Generally, a narrow pore is required for driving off large ions or solutes and selectively allowing only water molecules to enter then forming an uninterrupted single wire or clusters within pore confined conditions. Several classes of artificial water channels, including self-assembled channels, organic cages, carbon-based nanopores, aromatic foldamers, pillar[n]arenes, and macrocycles have been systematically outlined in this review in terms of their structural properties and transport mechanism. Additionally, molecular simulation analysis can be applied to verify the spatial atomic distribution of channels, importantly it enables to reveal a deep understanding of the arrangement of water molecules within these pores. Herein, this review will introduce the recent achievements in artificial water channels listing how the astonishing examples operate in the presence of water molecules, and it may arouse more inspiring views for the continued research in the field of water selective channel-forming assemblies and their application in the field of membranes for water purification.

© 2014 xxxxxxxx. Hosting by Elsevier B.V. All rights reserved.

1. Introduction

Water is one of the simplest molecules in the universe, but there are still great challenges for determining the precise role of its superstructures interacting and determining the function of biologically active molecules. A single water molecule composed of a central oxygen connected to two hydrogen atoms presenting an angle of 104° it is a dipolar molecule that can associate with other water molecules *via* donor-acceptor hydrogen bonds. A fascinating most perfect water assembly created by nature is solid ice, a stiff supramolecular material completely cross-linked by hydrogen bonds [1]. Free water and bound water play a major role in maintaining active functions of life [2–5]. Despite important advancements, a few unanswered questions are still attracting attention: how do water molecules collectively/selectively cross the cell bilayer membrane barrier? What is the selective mechanism for their distribution and transportation? What role do hydrogen bonds play in orchestrating the selective water vs. ions/protons translocation at the Ångström scale level?

The discovery of natural water channel proteins, the Aquaporins, has gradually led researchers to unravel the mystery of water translocation in living organisms. The diversity of their structural properties was recognized by the presence of different Aquaporin channels in different

* *Corresponding auuthor*.
E-mail address: mihail-dumitru.barboiu@umontpellier.fr

xxxx-xxxx/$ – see front matter © 2014 xxxxxxxx. Hosting by Elsevier B.V. All rights reserved.
http://dx.doi.org/10.1016/j.aebj.2014.10.012

organs or tissues. Some subclasses such as hAQP0, 1, 2, 4 and 5 enable to transport selectively water, while rejecting other ions [6–12], which can be attributed to the unique narrow selectivity filter, allowing only single water molecule translocation. When present to the channel entrance, water molecules can automatically adjust their adaptive binding and orientation, followed by the generation of the continuous water wire/clusters through the channel. This process will be accompanied by the translocation of several small solutes when it comes to the subclasses of hAQP3, 7, 9, and 10 [13–16]. For instance, hAQP3 ships urea, glycerol, and water molecules. Additionally, the binding of Ni^{2+} with histidine 241 in hAQP3 can bring the Ni^{2+} sensitivity which is related to human lung diseases [17].

The water *vs.* ion/molecule transport selectivity offers the intriguing possibility of achieving important membrane separations on a large scale for environmental applications, such as water purification and desalination. However, it is difficult to maintain the protein activity of each AQP subunit under harsh pressure and salinity conditions used for these industrial applications. To date, high amounts of AqpZ from bacteria cells can be produced by virtue of gene engineering. The most used approach is to transfer the AQP-encoded plasmid to the bacteria cells as a result of the over-expression of recombinant AqpZ [18–20]. Researchers have already come up with a His-tag modification method that can help solve the problem of low yield. This breakthrough can offer the direct use of AqpZ in the membrane filtration field. Tang and co-workers have recently optimized the AqpZ loading in order to obtain the optimal membrane performance. They varied the protein-to-lipid ratio, vesicle loading, and supplemental cholesterol in a thin-film composite membrane, showing a reliable standard for practical application [21].

In parallel, the discovery of artificial water channels - the synthetic counterparts of Aquaporins - busted the researchers' efforts to develop selective biomimetic membranes for environmental application. The available diverse functional groups make it possible to decorate artificial channels and to have access to selective pathways for the diffusion of water. An increasingly growing number of novel compounds have been recently reported, leading to profound improvements in the transport performances of artificial water channels [22–29]. Small structural changes can make a huge difference in the construction of selective pores and can bring more diversities of these artificial alternatives used to sieve larger hydrated ions or molecules. Further structural details can be more precisely obtained from studies on their simpler X-ray single-crystal structures and molecular simulations. The hydrogen bond interactions of channel-water and water-water can help us understand the orientation and arrangement of water molecules within the channels, as well as learn the dynamic translocation process. Deep comprehension toward the water transport mechanism will lay the foundation for the research in future applications [30, 31].

This review will describe in detail the existing artificial water channels, and attempt to understand their transport mechanism on the basis of confined water structuration within self-assembled channel superstructures, dynamically connected at the Ångström scale. The mechanistic details might give a better understanding of the selective water transport behaviors, moreover may arouse an important understanding of the molecular design of biomimetic channel alternatives working as natural ones. Systematically, examples of organic cages, carbon nanotube porins, self-assembled channels, aromatic foldamers, pillar[n]arenes, and macrocycles will be presented below (Scheme 1). Some of them have been embedded into Reverse Osmose RO membranes and tested for the real desalination processes of seawater. Their unique spatial self-assembled superstructures allow water molecules to be arranged in well-organized ordered single-wires/clusters inside selective channels, thus making it intriguing for further development in the molecular separation field [32–36]. Therefore, this work will summarize the essence of current artificial water channels by listing their structural properties and elucidating the water permeation process, and it will envision to stimulate more ideas for practical applications.

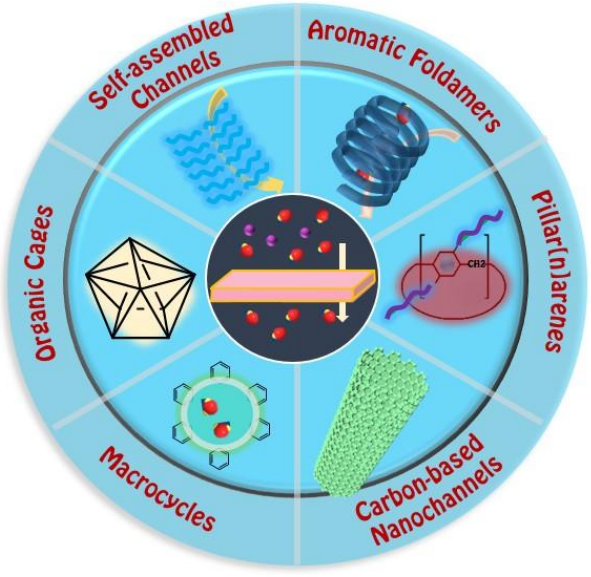

Scheme 1. Schematic representation of the existing classes of artificial water channels.

2. Natural porins for water/proton trafficking

To date, channel proteins are one of the most important transmembrane biomolecules discovered in living organisms. They allow specific molecules or ions to cross the bilayer membrane barriers. In this section, we will highlight the structural behaviors and transport mechanisms of several natural biological water channels: aquaporins, gramicidin A, influenza M2, etc., and extract the potential structural information leading to selective water transport useful for current environmental applications.

The aquaporin family shares a common basic six-transmembrane helices for the bidirectional water transfer, which is dependent on the continuous hydrogen-bonded networks among adjacent water molecules and inner channel components. Other small solutes can be transported across the bilayer, thus differentiating classical AQP or aquaglyceroporins. The amphoteric water allows the movement of protons *via* a Grotthuss mechanism [37,38], showing that protons may hop among neighboring water molecules to achieve fast transfer.

2.1. Aquaporins

As one of the nature crafts with exceptional water permeation, the aquaporins family has been discovered by Agre et al. [39,40]. Classified by their selective functions, thirteen mammalian aquaporins were identified into three subfamilies including orthodox aquaporins, unorthodox aquaporins, and aquaglyceroporins which are enable to permeate small solutes such as glycerol and urea [41]. In their transmembrane domain, two functional sites are critical for water transport selectively and effectively (Fig. 1a) [42,43]. Taking aquaglyceroporin GlpF as an example (Fig. 1b) [42], at the exit of the

channel, an aromatic/arginine (ar/R) constriction region filter with a 2.8 Å of diameter is big enough to allow one single water molecule passing and exclude ions and small solutes. Additionally, they have a unique central NPA (Asn-Pro-Ala) sequence allowing the neighboring waters to assemble with opposite dipolar orientations (Fig. 1b). At this narrowest site of the pore, one water is doubly connected *via* acceptor H-bonds to its oxygen atom with adjacent amino groups (Asn76 and Asn192) and *via* donor H-bonding of neighboring water molecules. The water orientation is rearranged in the NPA center, interrupting the possible path for proton Grotthuss diffusion, thus excluding the transport of protons along such opposite-oriented dipolar water wires (Fig. 1c). Without any other restriction of H-bonds, a minimal energy barrier can be easily surmounted across the narrowest pore, leading to fast water transport as well as proton preclusion assumed as H-bond isolation mechanism. In comparison, the more hydrophobic and 1 Å wider ar/R pocket in GlpF channel endowed the broader transport range towards not only water but also glycerol, urea, O_2, CO_2, and NH_3 [47,48].

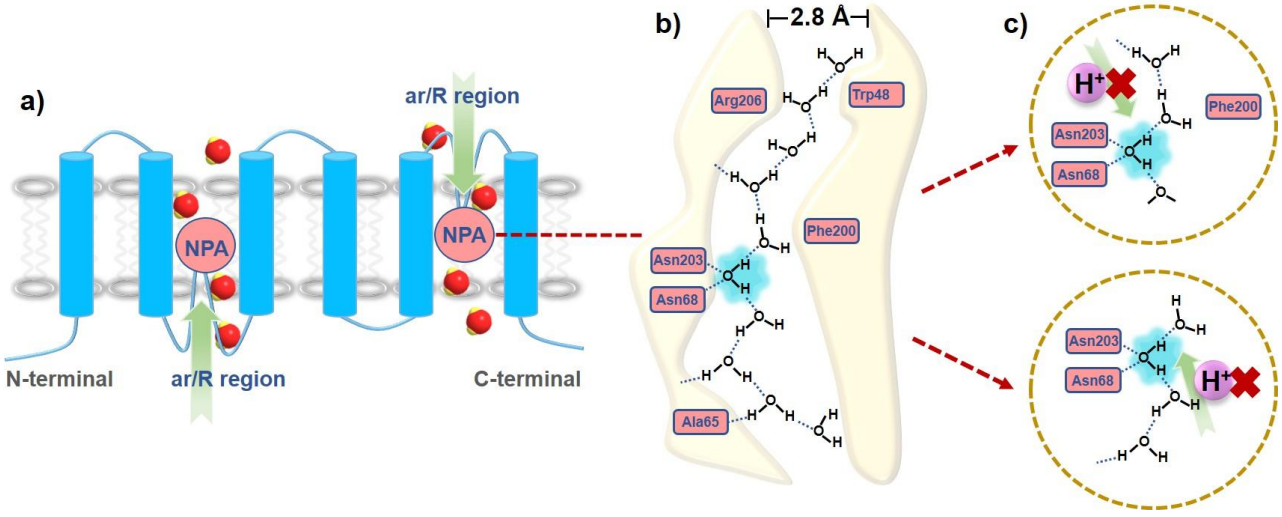

Fig. 1. a) Schematic representation of a common aquaporin topology of the six transmembrane α-helices, two functional sites containing the NPA center and ar/R region at reverse direction; b) the oriented water wire along the NPA region of the AQP pore center and c) the mechanism of proton preclusion along the narrowest pore region of the AQP. Reproduced with permission from Reference [42] Copyright © 2002 The American Association for the Advancement of Science and the permission from Reference [47] Copyright © 2008 National Academy of Science.

Having improved the scale-up production of aquaporins, one recombinant subtype AqpZ produced from *E.coli* was embedded into the membrane for desalination in scale-up fabrication [49–51]. Kumar has reported the first case of AqpZ-lipid-embedded PMOXAm-PDMSn-PMOXAm (ABA) triblock membrane at different AqpZ-to-lipid ratios [52], showing at least two orders of magnitude of enhanced water productivity compared to the reference membrane. Moreover, this work inspired the further optimization of AqpZ concentration in membrane [53], and also paved the way for the development of more potential AqpZ-embedded or MP (membrane protein)-inserted polymeric membrane (Fig. 2a) [54–56].

2.2. Gramicidin A

Gramicidin A is a pentadecapeptide with a narrow pore diameter of 4 Å for selective monovalent cations transport [57]. Differently from aquaporins, protons were conducted with a flow rate of 8 times higher compared to water movement, as a uniform single-file H-bonded water wire is present along the channel facilitating the proton hopping.

Molecular dynamic simulations showed that 22 waters can be accommodated inside the channel, H-bonded to the carbonyl oxygens of the wall surface [58]. In the middle of the channel, an excess proton was captured in the form of an $O_2H_5^+$ ion which can influence the water orientations but not in the channel conformation (Fig. 2b). Explained by the proton-wire mechanism, the proton had access to move rapidly along a confined channel which was determined as a 2.0-Å-radius of pore size with a small diffusion constant of water [59].

2.3. M2 influenza virus protein

M2 protein is a pH-regulated proton-selective channel from influenza A virus [60–62]. It contains a transmembrane (TM) region formed by four helical strands surrounding a narrow pore. It has been indicated that the pH-dependent proton transport performances can be attributed to the pKa of the imidazole ring along with its tautomerization [60]. Proposed by Hirata's group, the protonation states of two imidazoles were switched twice from protonated to non-protonated, and from non-protonated to protonated, as shown in Fig. 2c-2d. The δ-N site of neutral His-37 is protonated at lower pH, followed by the translocation to the Ɛ-N site for achieving proton transfer among water molecules [63]. On the other hand, the gate of the channel will be blocked at high pH as a result of the intermolecular interaction between Trp41 (W41) and Asp44 sites [64]. Further study demonstrates that the accommodation of water in the Ser31 site is vital for the proton conduction that can be regarded as a bridge to transmit a proton to the His37 site where a 1.7 Å of size constriction is located for precluding ions (Fig 2e).

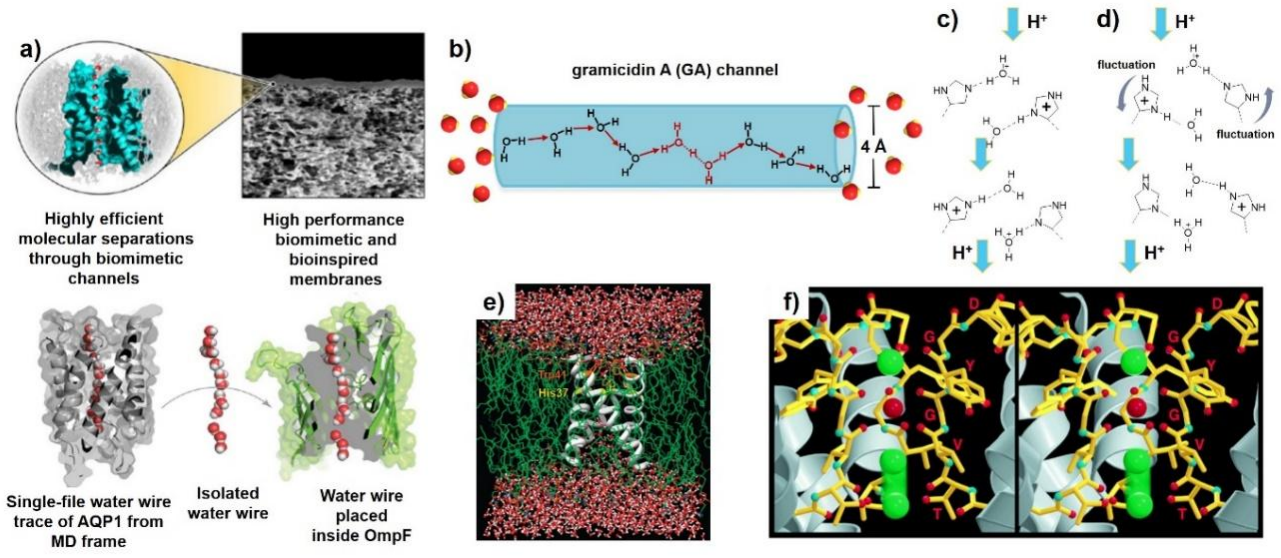

Fig. 2. (a) High performance RO Membrane embedding thef AqpZ (up), and simulated water wire within AQP1 pore which was then placed inside OmpF protein to study its dynamics ans stability(down). Reproduced with permission from Reference [55] Copyright © 2018 American Chemical Society, (b) Schematic representation of the gramicidin A channel with the presence of water molecules and a proton transport via elusive O_2H_5+ species (in red) along the channel. Reproduced with permission from Reference [58] Copyright © 1996 The Biophysical Society by Elsevier, (c) and (d) the proposed mechanism of proton transport along of M2 influenza channel. Reproduced with permission from Reference [63] Copyright © 2010 American Chemical Society, (e) the simulated M2 influenza tetramer in POPC lipid bilayer, showing the His37-filter and Trp41 gating. Reproduced with permission from Reference [63] Copyright © 2010 American Chemical Society, (f) the stereoview of KcsA channel selectivity filter showing the water-potassium sequences along the channel. Reproduced with permission from Reference [65] Copyright © 1998 The American Association for the Advancement of Science.

2.4. Binding site of water in ion channels

Generally, the accommodation and translocation of ions through natural proteins are dependent on the coordination behaviors replacing the native ion-hydrated states in bulk water. Taking advantage of the amphoteric function of the water molecule, it enables to be the site of coordination bond as well as channel-water hydrogen bond, wherefore assisting in performing the ion transport process. For instance, KcsA is a well-known channel protein with a 3 Å-diameter as a filter for selective K^+ transport [65,66]. Up to eight coordination bonds can be formed by KcsA -channel and K^+ -water linkages (Fig. 2f). Within the channel, it has been illustrated that the four binding sites were occupied equally by two potassium atoms and two water molecules coined as 1-3 and 2-4 configurations [67], herein water molecules play a vital role in connecting the adjacent K^+, meanwhile bonding to the channel wall.

2.5 Inspiration for artificial water channels

Nature has created remarkable channels for efficient and selective water transport as suggested by the examples of natural protein channels presented in this section. One common structural feature is the narrowest hollow close to 3 Ångström pore size, which is only slightly larger than a confined water molecule size. To the best of our knowledge, the hollow architecture can be provided by the original molecular configuration, for instance, the helical foldamers, and carbon nanotubes, or formed by the self-assembling tubular architectures through intermolecular interactions. Another important point is related to specific water-water and water-protein wall donor/acceptor H-bonding interactions able to stabilize confined clusters of water that might be responsible for the selectivity of the translocation. Charged moieties could play also a role in the rejection of ions but also are highly important for the orientation of channels within the bilayer membranes.

3. Artificial water channels

Inspired by natural protein channels, scientists have focused on the synthesis of artificial channels that allow water to transport selectively through a hollow architecture. The first synthetic self-assembled dendrimeric pore structure for water transport was reported by Percec et al. However, the water translocation within these pores was very low [68]. After that, several new artificial water channels have displayed excellent transport behavior close to aquaporin's level. Importantly, the mechanism involved in the intermolecular interaction deserves much attention for their further development as alternatives in water purification and desalination.

3.1. Water-assisted self-assembled channel

3.1.1. Imidazole-quartet channels

Barboiu et al. have reported the self-assembled functional I-quartet artificial water channels, showing the permeability of ~10^6 H_2O/s which is within two orders of magnitude of AQPs' rates (Fig. 3a) [69]. Along water wires, protons also can pass through the channel due to the unique dipolar orientation of water which results in strong dipole conservation. The dipolar orientation of water along the I-quartet channel is shown in Fig. 3a, the oxygen atom is strongly bonded to the imidazole N-H group as well as to vicinal water molecules with a distance of 1.92 Å and 1.94 Å, while the hydrogen atoms are bonded by both oxygen atom and the imidazole nitrogen atom (1.87 Å), as a result of the formation of water-

assisted 'open form'. With the absence of water molecules, the spatial distance between adjacent imidazoles at one side is decreased to 1.85 Å, while at the other side, 2.73 Å of hydrogen bond was still kept. It is of interest that an inversion center in the assembled channels leads to the reversion of dipolar orientation as shown in Fig. 3b. When it comes to the rigid bis-ureido containing compounds, the hydrogen bonds distribution becomes more alternative, which is attributed to the two possibilities of the occupancy in both opposite orientations of the water dipoles [70].

Additionally, the subsequent overall pores after varying the alkyl chains of I-quartet have the same diameter of 2.6 Å (Fig. 3a), this is reminiscent of natural aquaporin's 2.8-Å pore for the efficient water transport [69]. The alkylureido chains varied from butyl-, hexyl-, octyl-, dodecyl, or octadecyl- or between chiral S-octyl-, R-octyl- and achiral octyl- (Fig. 3c), showing obvious increasing correlations between self-assembly behaviors and water translocation by an order of magnitude. Furthermore, even if the high net permeability was determined in bilayer vesicles, the incorporation of I-quartet AWCs with longer alkyl chains would lead to an easy precipitation of hydrophobic aggregates and the formation of defects in the polymeric membrane layer. Practically, hexyl I-quartet, HC6 presents an optimal choice over other alternatives concerning the water transport ability of the single channels or their solubility in the bilayer membranes or in polymeric films where a high-density distribution is requested for water permeation over the surface membrane but not affecting the mechanical stability of membranes. Multichannel crystalline or sponge-like HCx clusters were observed, displaying the presence and transport of water, as well as the H-bonding connection among them through MD simulation [71].

Highly selective ultrapermeable polyamide I quartet AWC membranes have been prepared fabricated and tested under real desalination seawater desalination conditions at the industrial scale (Fig. 3c). Improved permselectivity has been obtained leading to important energy reduction [143, 144].

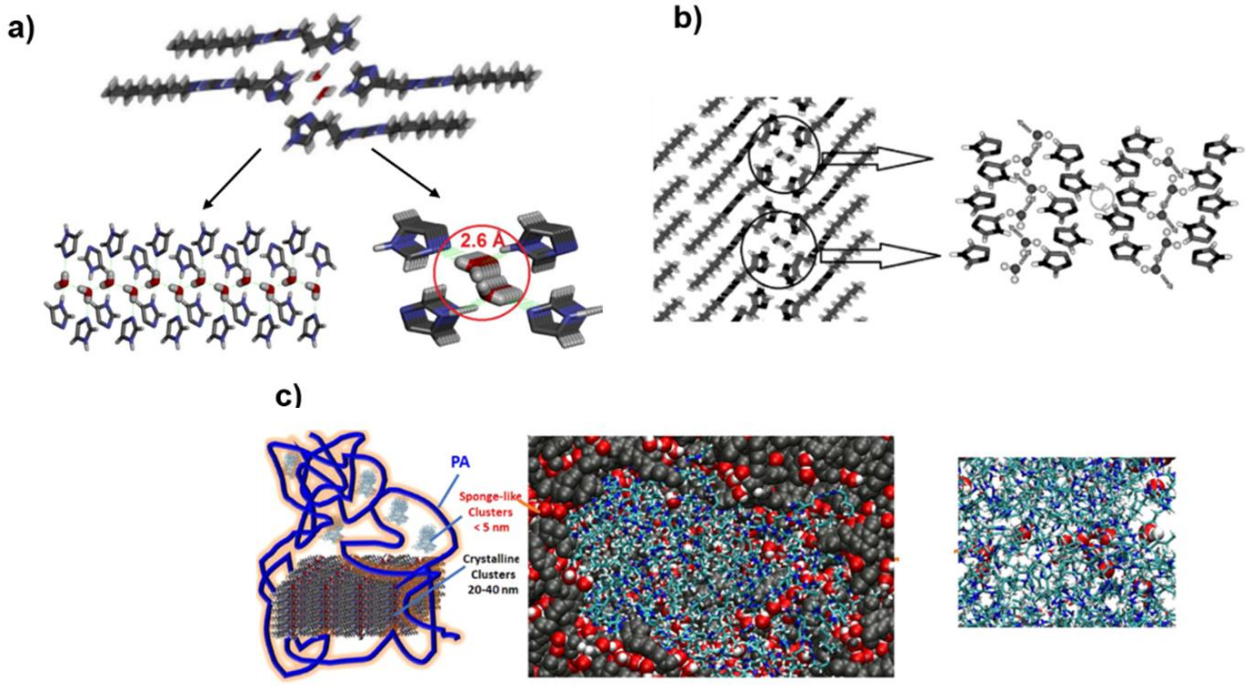

Fig. 3. (a)) The crystal structure of I-quartet channel with a diameter of 2.6 Å and (b) dipolar orientation of water wires within the channels presenting an inversion center. Reproduced with permission from Reference [69] Copyright © 2016 American Chemical Society, Reference [70] Copyright © 2011 WILEY-VCH Verlag GmbH & Co., Weinheim; (c) Molecular simulation study of I quartet crystal structure embedded within a polyamide membrane matrix. Reproduced with permission from Reference [71] Copyright © 2021 American Chemical Society.

3.1.2. Hydroxy channels

Inspired by the ceramide channels, Barboiu et al. described the OH channels by combining alkylureido arms with hydroxylic ethanol, propanediol, and trimethanol water binding components, presenting a high affinity for water [72]. The OH channels provide the bulk donors-acceptors H-bonding environment for the formation of water wires or clusters along the assembled channel or pore as the function of concentration (**Fig. 4a-4c**).

No water molecules were observed in the single crystals of OH-channels. However, strong concentration-dependent water transport behaviors were observed for these compounds in which the H-bonding networks can be observed by water cluster formation within larger channels in bilayer membranes. The AQP-level water net permeability enables the authors to emphasize the efficient transport mechanisms *via* transient water wires and sponges in larger channel superstructures, meanwhile displaying high ion or proton rejection.

The water sponges in larger channels show two orders of magnitude higher water permeability than that of water-wires. The detailed MD simulation was performed to explain the membrane-embedded artificial channel structures, as shown in Fig. 4c the three regimes of channel H1 including spongelike, crystal-like, and dissolved form are stabilized in the membrane. Then, Pasban and coworkers [73] have carried out molecular dynamic simulations and well-tempered metadynamics simulations to reveal the water permeability of hydroxy channels in the presence of different ions including nitrate (NO_3^-), magnesium (Mg^{2+}) and calcium (Ca^{2+}) as shown in Fig. 4d. It was indicated that the water transport behaviors may be dependent of the size of small ions, as well as the active

site of artificial channels that in this case the hydroxy group can help to absorb and stabilize water clusters and swell inside the pores.

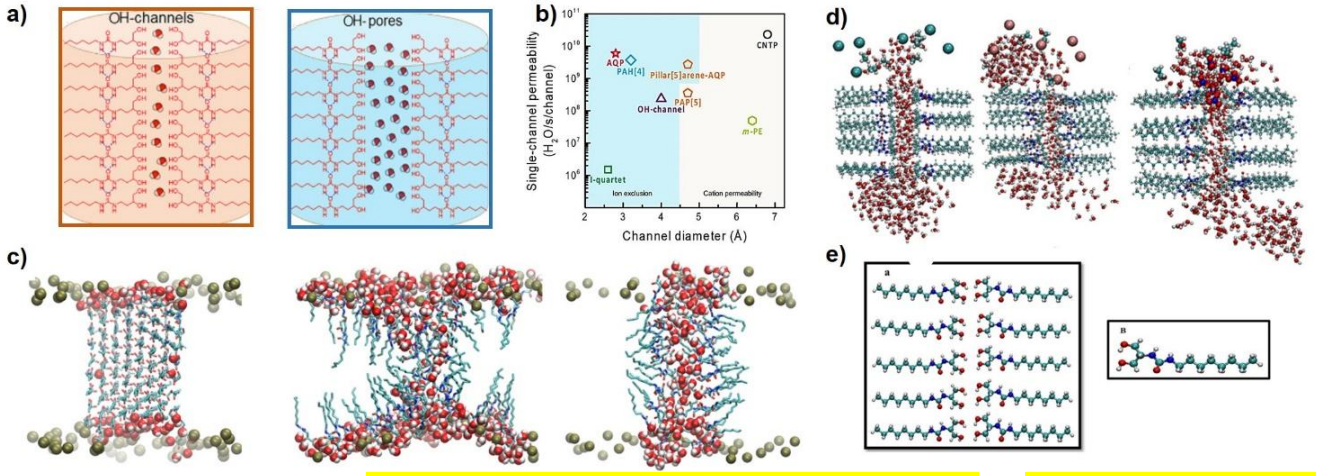

Fig. 4. (a) Chemical structures of hydroxyl channels or pores embedding single water -wires or clusters respectively; (b) The single-channel permeability of representative artificial unimolecular pillararene PAP[4], Pilar AQP PAP[5] and self-assembled I quartet and hydroxy water channels compared with the AQPs channels; (c) MD simulation of hydroxy channel H1 and the formation of adaptive water clusters in the bilayer membrane. Reproduced with permission from Reference [72] Copyright © 2021 American Chemical Society; Metadynamic simulations of a hydroxy channel (d) with the presence of different ions, (e) detail of the self-assembed of free water hydroxy channel. Reproduced with permission from Reference [73] Copyright © 2023 Springer Nature.

3.1.3. Peptide-diol channel

Talukdar et al. have reported a series of peptide-diols combining L-phenylalanine and D-mannitol connected to two aliphatic chains (Fig. 5) [74]. Dual water wires along the diol segment were observed in the crystal structure, with a strong H-bonding between $O_{(water)}$-$H_{(diol\ OH)}$, $H_{(water)}$-$O_{(diol\ OH)}$, and $H_{(water)}$-$O_{(amide\ C=O)}$, but surprisingly with any interaction among water molecules. The intricate alternative H-bonding between channel OH groups and water allows the accommodation of water within a diameter of 2.5 Å, thus leading to the superfast transport behavior. Our opinion is that the hydroxy channels are very adaptive examples of selective channels stabilizing in a very effective manner the cluster formation and synergistic water translocation

3.1.4. Diphenyl-hydroxy helix

A hydroxyl-based self-assembled water channel was obtained with the self-assembly of a hydrophobic diphenyl segment (Fig. 6a) [75]. The six stacks of 2-hydroxy-N-(diphenylmethyl)acetamide HNDPA units created a hollow cylindrical architecture where an inner helical water wire was present along the tubular path and stabilized via donor H-bonding with assembled $(OH)_6$ supramolecular hexagons. The water occupancy under a large temperature gap from 110 K to 350 K, indicated that the low temperature may make a big difference in the stability of the channel structure resulting in the decrease of water content. This channel remains an optimal model as the water transport remains to be proven.

3.1.5. Bola-amphiphile-triazole channels

Barboiu et al. have reported a class of synthetic triazole TCT non-selective ion/water channels [76,77]. It was indicated that TCT had similar transport behaviors and performance to gramicidin A, conducting water and proton while selective to cation/anion. Two hydrogen bonding positions happen to –NH---O_{H2O} and –C=O---H_{H2O} which are verified by X-ray crystal observation. Within the 5 Å-diameter of the channel, water clusters are divided into two layers at opposite directions, showing that two wires are close to the inner channel surface by the H-bond interaction (Fig. 6b-6c). Additionally, the translocation of alkali cations was attributed to hydration-dehydration processes along surrounding water molecules dynamically H-bonded to cover the inner wall of the channel. Our opinion is that this hydrophilic channel design is one of the innovative way to construct adaptive dynamic channels for selective translocation.

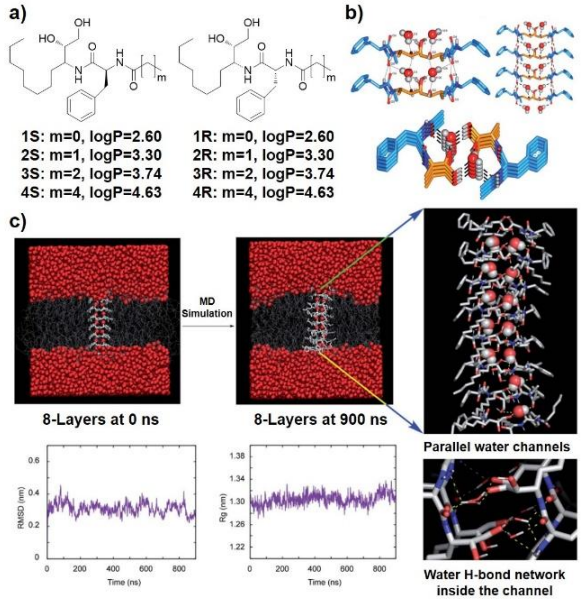

Fig. 5. (a) Peptide-diol molecules and (b) their crystal structure showing the formation of H-bonded water wires within the channel, (c) the snapshot from MD simulation of the 4R channel showing the water H-bonded network. Reproduced with permission from Reference [74] Copyright © 2022 The Royal Society of Chemistry.

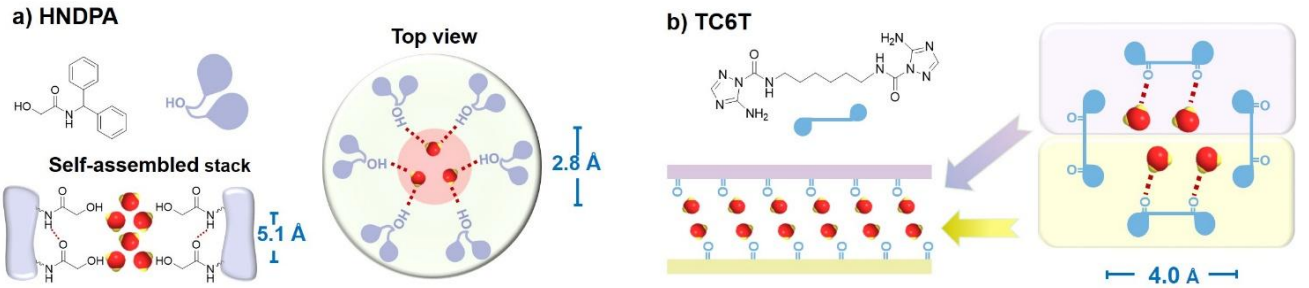

Fig. 6. (a) Schematic representation of supramolecular diphenyl-hydroxy helical supramolecular channel. Reproduced with permission from Reference [75] Copyright © 2022 Wiley-VCH GmbH; (b) Schematic representation of bola-amphiphile-triazole TCT channel, and the water distribution along the channel. Reproduced with permission from Reference [77] Copyright © 2014 Springer Nature.

3.2. Aromatic foldamers

Aromatic foldamers have been studied for more than two decades due to their highly functional biomimetic hydrogen-bonded-stacked helical architectures. Easily available starting materials are used as monomers for the formation of foldamer backbones, providing extensive hydrogen bonds and aromatic stacking interactions for stabilizing the folded conformations [78,79]. This set of hollow helical shapes with inner channel architectures gave inspiration to the development of water/ion channels. The selection of helical units plays a vital role in forming an adapted and precise hollow structure for achieving selective transport functions. It is attributed to the possibility to selectively build different cavity sizes and to structurally design a optimal inner distribution of variable binding sites at the Ångström scale, leading to selective binding with ionic or molecular species.

3.2.1. Polypyridine foldamer

Zeng's group have reported a class of short foldamers with ''sticky end'' which contributed to the helical stacking through electrostatic interactions [80–82]. The single foldamer contains five or six repeating units named pentamer or hexamer, and it is sufficient enough to form a helical turn using 4.3 residues [83].

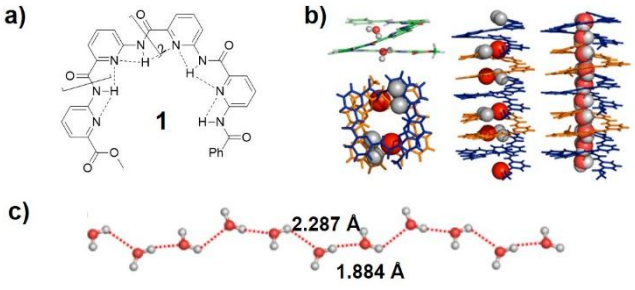

Fig. 7. (a) Structure of the pentameric foldamer **1** and intramolecular hydrogen bonding leading to foldameric channels; (b) the helical stacks in the crystal structure of pentamer **1**; (c) A H-bonded 1D water chain as extracted from the crystal structures of foldamer **1**. Reproduced with permission from Reference [84] Copyright © 2014 American Chemical Society.

While in this work, they demonstrated that the sticky ends do not always help to form the helical stacks, other factors including surface over protrusion, stronger intermolecular hydrogen bonds, and shorter single foldamers may interfere with the packing states [84]. The pentamer **4** grafted with an ester end and phenyl ring [85] present the 1D helical chiral stacks *via* intercolumnar edge-to-edge contacts as shown in Fig. 7a-7b. Four water molecules were accommodated in each turn, and the single wire was generated through the H-bonds among water molecules, where one water was stabilized by another two neighboring waters (Fig. 7c). Additionally, five H-bonds were formed between water dimer and the inner surface of **1**.

Several novel pentamers **2** and **3** (Fig. 8a) containing a phenyl ring were subsequently designed [86]. A small elongation between the phenyl ring and pyridine unit brings an average diameter of 2.8 Å, showing the weaker binding of **2** to water, thereby resulting in the faster water transport rate (~$3*10^9$ H_2O/s/channel). Assumed from the crystal structures of **2**·$(2H_2O)_n$ and **3**·$(2H_2O)_n$, the enhanced water flow rate can be attributed to the more optimized position of water molecules accommodating inside the channel as well as the more spacious space for translation and rotation (Fig. 8b).

Furthermore, the authors have synthesized the polypyridine-based aromatic folded pentamer through one-pot polymerization using $POCl_3$, showing an average length of 2.8 nm as a breakthrough [87]. About the largest polypyridine amide foldamer P31 (Fig. 8c), the 31 of repeating N-H in the channel allows the formation of H-bonds of channel-water and water-water [88], as a result, creating a single-file water wire along the hollow cavity for water and proton transport as shown in Fig. 8c. The flow rate of channel P31 can reach at $1.6*10^9$ water molecules/s/ channel, as well as proton permeation at the gramicidin A scale.

3.2.2. Pyridine-pyridone foldamer

Pyridine and pyridone moieties have been used to obtain polymeric foldamers by varying the coupling agents, (Fig. 8d) [89]. The use of pyridone units enabled to form three types of hydrogen bonds including C=O---H-O-H---O=C, C=O---H-O-H---$N_{pyridine}$ and $N_{pyridine}$---H-O-H---$N_{pyridine}$, which means that no extra H atom can be bound to the O atom in the neighboring water, thus leading to the bifurcated H-bonds and the disrupted water wires (Fig. 8e). The further binding of protons into the channel, 2-3 Å or slightly more, may promote the connection of two short water chains, generating a fully H-bonded water chain for proton transport *via* the Grotthuss mechanism.

3.2.3. Quinoline helix

Liu and coworkers have reported a class of quinoline-based helical foldamers **4** as the proton channels [90]. The number of repeating units is varied from 4 to 16, thus obtaining 4 mer, 8 mer, and 16 mer of different lengths respectively (**Fig. 9a-9c**). A small luminal cavity with a diameter of only 1 Å allows the helix to preclude ions and water except for protons. Different from other water wire-assisted proton channels, the fast exchange between protons of active NH and N-pyridine groups inside the hollow cavity and protons assisted by the water molecules at the two ends was able to trigger a single-file proton wire.

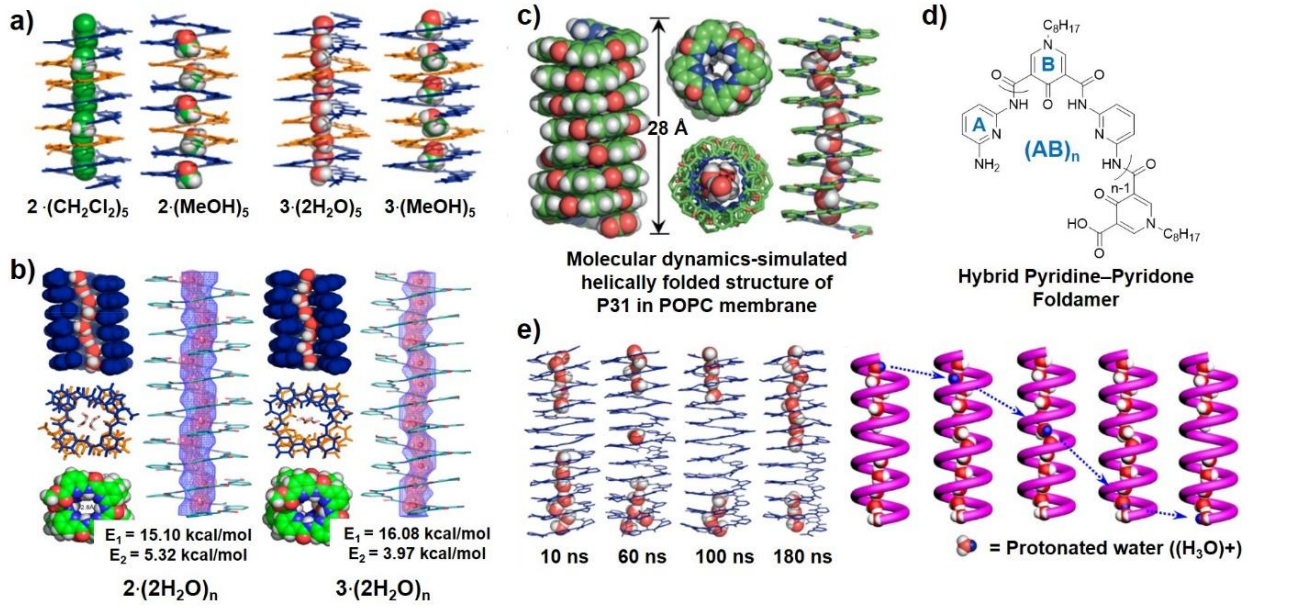

Fig. 8. (a) Crystal structures of polypyridine-folded pentamer **2** forming a 1D chain of dichloromethane (CH_2Cl_2) or methanol (MeOH) molecules, and pentamer **3** forming a 1D chain of water or MeOH molecules; (b) Crystal structures of aquafoldamers 2·(2H_2O)n and 3·(2H_2O)n. Reproduced with permission from Reference [86] Copyright © 2020 American Chemical Society; (c) Molecular dynamic-simulations of P31 foldamer encapsulating a water wire; (d) The chemical structure of hybrid pyridine-pyridone foldamer; (e) The proposed mechanism of proton transport along water wires for channel (AB)25. Reference [87] Copyright © 2020 WILEY-VCH Verlag GmbH & Co. KgaA, Weinheim, Reference [89] Copyright © 2022 WILEY-VCH GmbH.

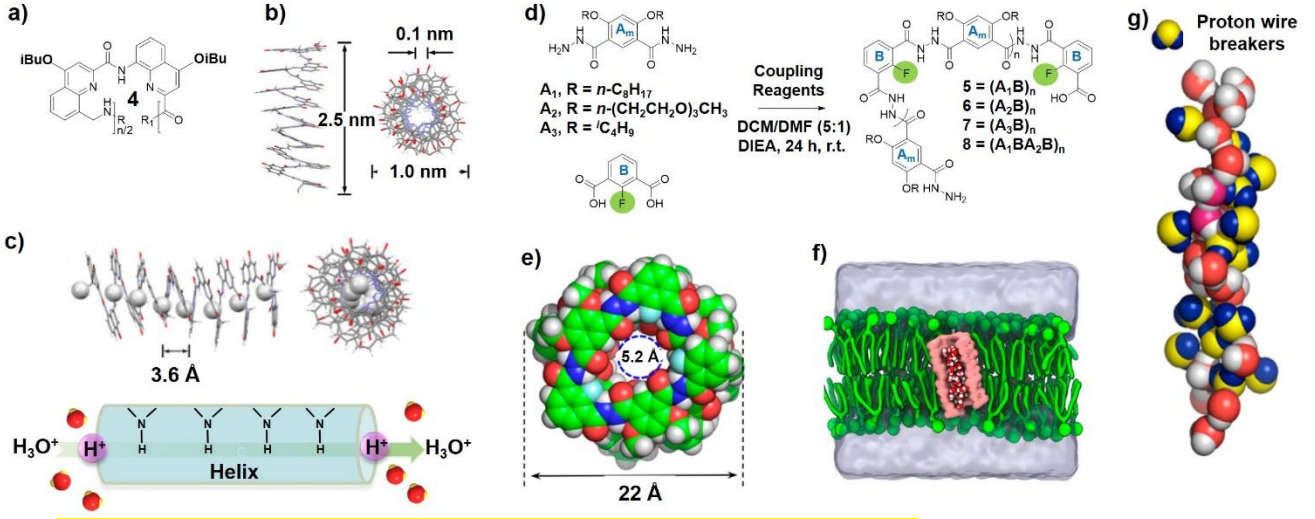

Fig. 9. (a) Chemical and (b) single-crystal structures of quinoline helical foldameric channel **4** for proton transport; (c) The mechanism of proton transport along the quinoline-based helix inner surface. Reproduced with permission from Reference [90] Copyright © 2021 American Chemical Society; (d) The proposed synthetic route of fluorofoldamer by one-pot polymerization strategy; (e) Helical tubular structure of (A1B)8 oligomer by QM-computation and (f) insertion of the water-containing channel in POPC lipid bilayer; (g) The distribution of proton wire breakers within the water clusters. Reproduced with permission from Reference [92] Copyright © 2022 American Chemical Society.

3.2.4. Polyacylhydrazone foldamer

A series of polyacylhydrazone foldameric water channels were readily obtained by using the one-pot polymerization method and varied coupling reagents [91]. The QM-optimized pore structures have indicated that tunning the inner groups made a big difference in the cavity size, channel **7**-LA and **8**-LA have a sizable cavity of 6.5 Å and 4.5 Å for water accommodation, whereas the diameter of channel 5 is 3.0 Å due to the block of isopropyl group. This example show that variable inner diameter can be created within different structures that are useful to explain different transport mecanisms at different scales. Inside the cavity of **7**-LA and **8**-LA, around 48 and 33 water molecules were observed, respectively while about 36% of them belong to proton wire breakers, which means that these water molecules either form only one H-bond, or no bond, or form two H bonds *via* H atom or O atom therefore impeding the hopping of protons along water clusters.

Moreover, foldamers decorated with fluor atoms [92] were designed for fast water transport (Fig. 9d-9g). They have a pore size of 5.2 Å and a channel length of 2.8 nm for the accommodation of water clusters, displaying an ultrafast flow rate of $1.4*10^{10}$ water molecules/s/channel with an average of 40.7% proton wire breakers as well as high ion rejection. It was indicated that the introduction of C(sp2)-F brings dipolar bonds, good hydrophobicity, smaller cavity size, and weaker H-bonding capability which were regarded as vital factors for excellent water transport performances.

3.3. Macrocyclic channels

Macrocycles possess the inherent advantage of separating various sizable species compatible and selectively bound within their molecular diameters. Macrocyclic aromatic or peptide systems [93, 94] are self-assembled to tubular configurations through intermolecular H-bond or stacking interactions resulting in the formation of cylindrical or toroidal pores for fast permeation of ions or molecules.

3.3.1. Hexa(m-phenylene ethynylene) macrocycles

Gong and coworkers have designed a rigid macrocycle that can self-assemble to a nanotubular architecture by hydrogen bonds and π-π stacking for water transport [95]. By calculating the stacking angle and energy configuration, an optimal spatial arrangement was obtained once the relative stacking angle of two macrocycles was 19.5° and the subsequent vertical distance was 3.46 Å. The hydrophobic nanopore was determined at a diameter of 8.63 Å, having an aquaporin-level water transport with 22% of the permeability of AQP1. This work pioneered the design of macrocycles with hydrophobic nanopores for efficient water permeation.

3.3.2. Diethynyl-benzene-phenylene ethynylene hybrid macrocycle

Following this, a hybrid shape-persistent macrocycle was introduced by the Gong group [96], consisting of alternate hydrophobic and hydrophilic moieties, which take advantage of accommodating water clusters through the hydrogen bonding of water molecules and carbonyl oxygens. This anionic lumen allows ion-dependent water transport, Na^+ having the longest lifetime of its first-shell water clusters thus the lowest water permeability.

3.3.3. Tetra(ethylene glycol)-based discotic molecule

Wang's group synthesized a class of amphiphilic discotic molecules formed by tetra(ethylene glycol) chains and 12 dodecyl chains *via* Steglich esterification [97]. With the presence of water molecules as oriented directional templating guests (Fig. 10a-10c), these amphiphilic units can self-assemble to the well-aligned array, transporting water along the water-induced growth direction.

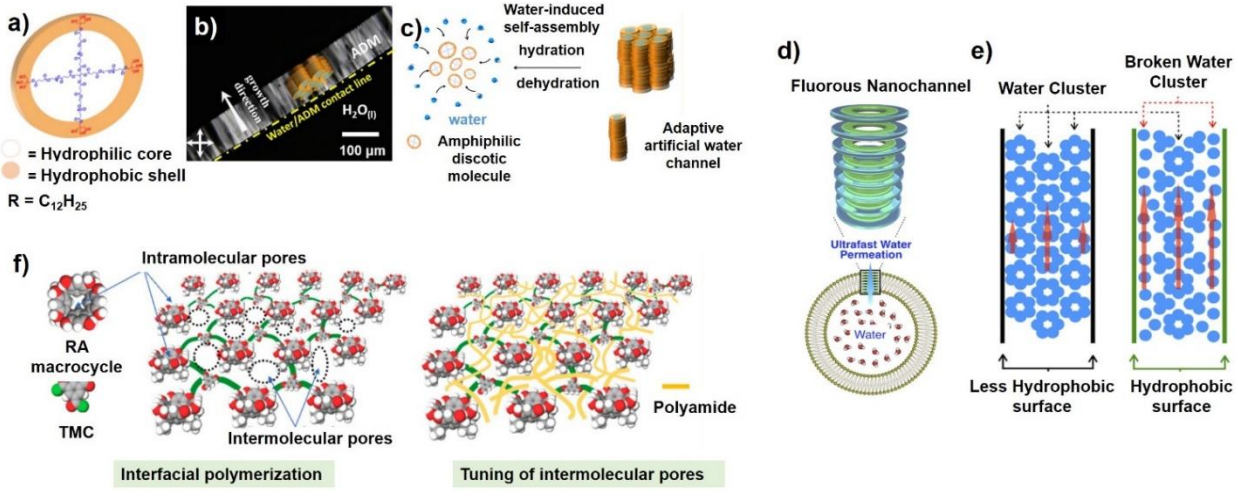

Fig. 10. (a) The chemical structure of amphiphilic discotic molecules used for (b,c) the directional growth of aligned mesophases within alumina ADM membranes for directional water transport and their dynamic transformation via water-induced self-assembly. Reproduced with permission from Reference [97] Copyright © 2021 American Chemical Society; (d) The schematic representation of fluorous macrocyclic nanochannels used for water transport; (e) The effect of fluorous matrix nanochannels inner surface on water clusters stability within channels. Reproduced with permission from Reference [98] Copyright © 2022 The American Association for the Advancement of Science; (f) Tuning the intermolecular pores in resorcin[4]arene membranes via interfacial polymerization. Reproduced with permission from Reference [100] Copyright © 2020 Elsevier.

3.3.4. Fluorine-modified macrocycles

Aida and coworkers have developed a class of fluorine oligoamide macrocycles [98] able to form water channels having stacked macrocyclic structures, required for narrow accommodation water clusters (Fig. 10d-10e). Furthermore, the authors were able to control the diameters of the lumen by tuning the amount of aromatic units, ranging from 0.9 nm to 1.9 nm. The hydrophobic surface can get rid of water H-bonding to the inner surface, leading to the fast delivery of water clusters through the nanochannels. Meanwhile, involving multiple fluorine atoms can generate a negative interior surface as the electrostatic barrier for ultrafast water permeation according to the computationally prediction

3.3.5. Arylene ethynylene macrocycle

Arylene ethynylene macrocycles can pile up to a uniform hollow channel, along with the multiple presentations of H-bonding of side chains and π-π stacking interactions [99]. The inner distribution was simulated, presenting a 1.1 nm diameter which packed up to three water molecules per layer. Compared to the previous case [93], this work demonstrated a broader pattern of 2-3-2-3 water molecules at each macrocyclic plane for higher water content. Even though the inability of efficient water transport, further modification of inner groups may improve the water channel performances.

3.3.6. Tetra-C-ethyl resorcin[4]arene

Prior to the real utilization in nanofiltration, many macrocycles have been studied with regard to the theoretical transport performance and mechanism. A direct incorporation of tetra-C-ethyl resorcin[4] arene macrocycles [100] into a cross-linked polymeric membrane was performed through interfacial polymerization (Fig. 10f), resulting in a high water permeability of 42.3 L/m^2/h/bar and sodium sulfate rejection of 96.5%. This work will inspire more possibilities in macrocycle-based materials for water purification areas.

3.4. Pillar[n]arenes water channels

Pillar[n]arenes were first reported by Ogoshi in 2008. The unique pillar-shaped structure was constructed by connecting the 1,4-dialkoxy-benzene units using a methylene bridge [101]. Then the construction of a tubular channel structure along the column axle can be performed by using lateral arms connected to Pillar[n]arene scaffold (Fig. 11a, **9** and **10**) [102,103].

Hou et al. have initiated the studies on pillar[5]arenes artificial water channels and these channels are also the very first representative examples of Artificial Water Channels [104]. Two overlapping self-assembled superstructures were observed through discrete crystal structures of compound **10**, it was piled up either uniformly or with a rotation angle of 36° in order to form a hollow cavity templated by a single-file water wire in both cases (Fig. 11b-11c). Eight water molecules were encapsulated inside each module, generating the H-bonded water chain during the crystallization process of the pillar scaffold. It was revealed that the conversion between the two modes happened in different solvents, **10a**→**10b** in ethylene glycol and **10b**→**10a** in methanol. The slight rotation of **10** may lead to the interruption of proton jumping, thus reducing or even stopping the proton transfer.

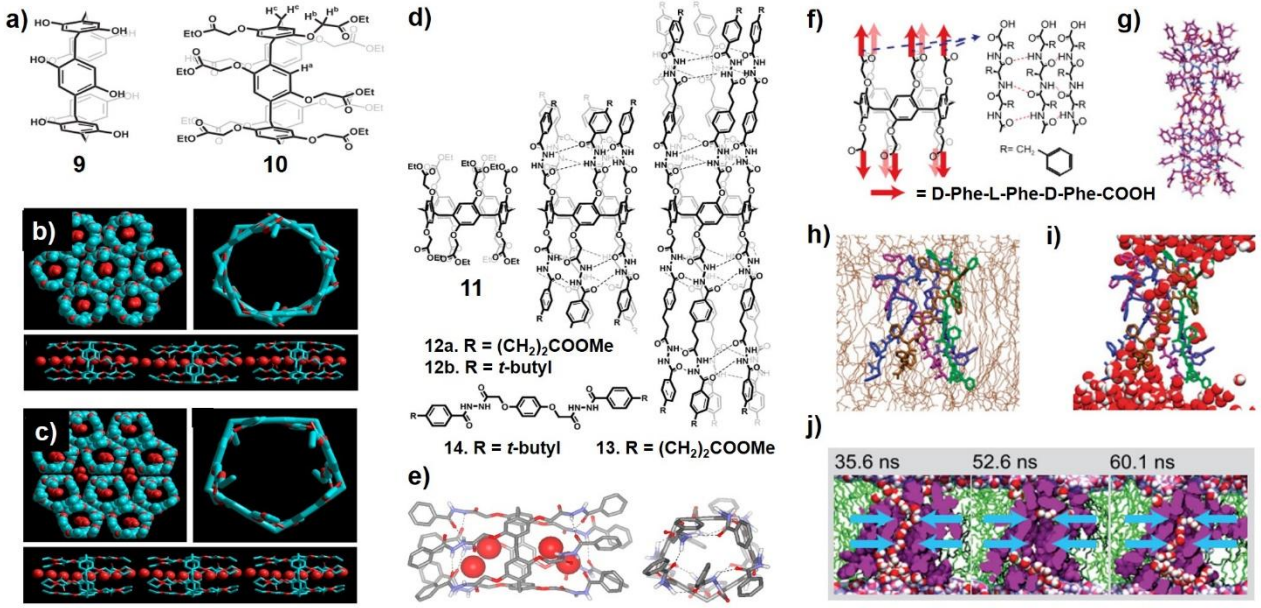

Fig. 11. (a) The chemical structure of pillar[5]arene **9** and its pillar[5]arene methyl ester **10** used for the design of artificial water channels; (b) and (c) the crystal stacking modes of compound **10** along the channel axis with encapsulated water molecules. Reproduced with permission from Reference [103] Copyright © 2010 American Chemical Society, Reference [104] Copyright © 2011 Elsevier; (d) The chemical structures of Hydrazide appended pillar[5]arene cylinders with varied

length and side groups; (e) The crystal structures of channel 12b with encapsulated water molecules. Reproduced with permission from Reference [105] Copyright © 2012 American Chemical Society; (f) The chemical structures of tripeptide-modified pillar[5]arene PAP; (g) The molecular model of unimolecular PAP molecule; (h) and (i) the simulated PAP channel embedded within a POPC bilayer; (j) MD simulations of the wetting/dewetting mechanisms of a PAP channels within bilayer membranes. Reproduced with permission from Reference [106] Copyright © 2015 National Academy of Science; Reference [106] Copyright © 2018 Springer Nature.

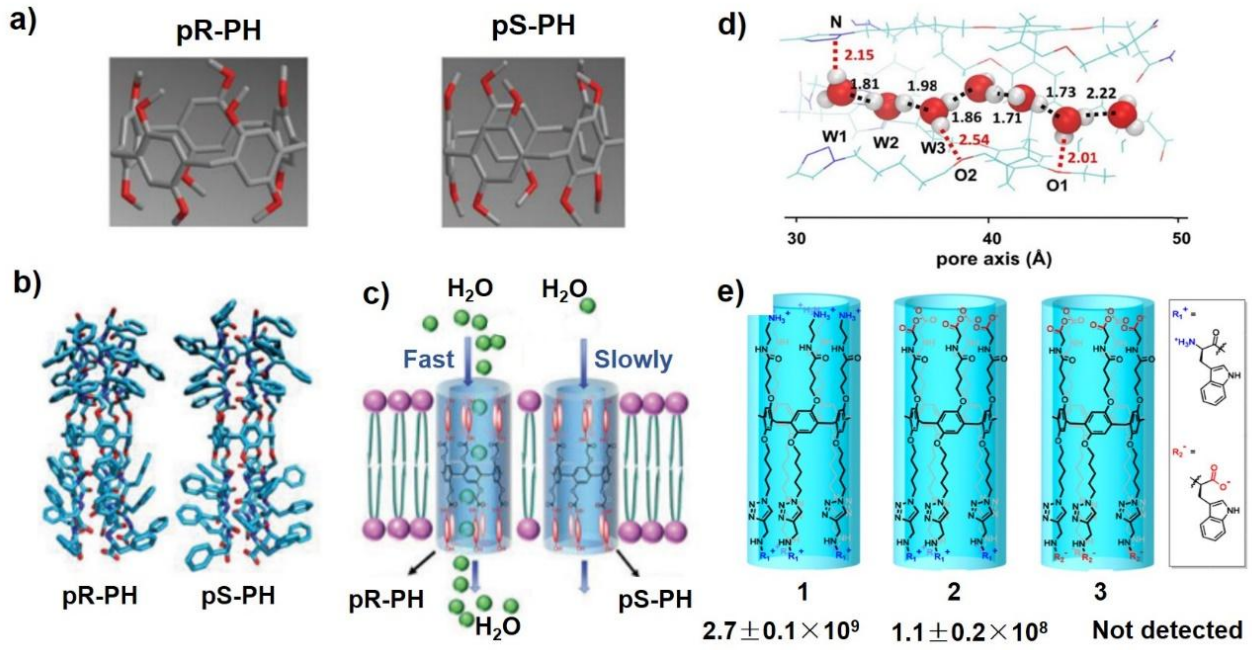

Fig. 12. (a) The crystal structures of diastereomeric pillar[5]arene pR-PH and pS-PH and (b) molecular dynamics simulated structures of from peptide-attached pillar[5]arene channels; (c) The water transport performances of pR-PH and pS-PH as observed in bilayer membranes Reproduced with permission from Reference [108] Copyright © 2019 WILEY-VCH Verlag GmbH & Co. KgaA Weinheim; (d) The inner interaction between the single-file water wire and pillar[5] arene AAQPs; (e) Chemical structures of AAQPs pillar[5]arenes with different charges: positive charges, negative charges and zwitterionic charges. Reproduced with permission from Reference [110] Copyright © 2020 American Chemical Society.

3.4.1. Hydrazide-appended pillar[5]arene

Taking advantage of the readily synthesis and available modification, Li and coworkers have reported a series of short or long-side chains hydrazide-appended pillar[5]arenes containing two or four benzene units, respectively on the central scaffold [105]. The eight intramolecular hydrogen bonds and two intermolecular hydrogen bonds between –NH and –C=O gave rise to the generation of pentameric cylinders. From the crystal structure of **12b** (Fig. 11d), it was shown in Fig. 11e that four water molecules were bonded to hydrazide groups inside the hydrophilic region of the channel.

3.4.2. Peptide-appended pillar[5]arene (PAP)

The involvement of intramolecular hydrogen bonds is regarded as a vital factor for the stabilization of long pillar structures. Thus the peptide scaffolds grafted with the pillar scaffold attracted much attention as the H-bond forming and membrane inserting hydrophobic components. The D-L-D poly-phenylalanine $(Phe)_3$ modified pillar[5]arene was reported by Hu et al. in 2015 (Fig. 11f) [106]. It has been demonstrated by molecular modelling that the aromatic rings of side chains were extended outside of the tubular structure allowing water molecules to permeate through the PAP channel with an average pore of 5 Å, without ionic selectivity. Important wetting-dewetting transitions happened to the channel with the presence of 30 % full-water wetting hydrophobic channels in a lipid environment (Fig. 11j). Additionally, the length of the PAP channel is around 4 nm which is favorable for the insertion in a bilayer membrane system [107].

In the consideration of the chirality of pillar[5]arene, two isomers (pS and pR) were evaluated from two facets --- inner structure and transport activity (Fig. 12a-12c) [108]. Both isomers enable to form a hollow structure, the only difference is the relative orientation of side chains. Interesting chiral pressure may induce a selective water transport performance of the pR channel in comparison to the pS channel in lipid membrane environments. The direct inclusion of such selective liposomes embedded via interfacial polymerization in solid polyamide membranes was evaluated by Wang et al. for seawater desalination [109].

3.4.3. Artificial AAQP pillar[5]arene

It was recently shown that pillar[5]arene AWCs can be used to treat AQP-related diseases by efficiently using these channels as artificial AAQPs in cell membranes by Hou et al. [110] AAQP can work in bilayer membranes to allow a water permeability close to that of AQPs and simultaneous ion and proton exclusion. The AAQP was constructed from tubular pillararenes containing positively charged rims, hourglass-like cavities and pore constrictions to generate steric hindrance. As a proton acceptor, a triazole moiety was found to interact with water molecules within the pillar[5]arene, discontinuing the formation of proton wire,

reminiscent of the natural AQP channel mechanism [110]. The narrow pore allows only one water molecule to pass, thus generating the single-file water wire with three remarkable H-bonds between water and channel inner surface, H_{H2O}---$N_{triazole}$, H_{H2O}---$O_{(-O-)}$ (Fig. 12d). The authors have revealed that different positive, negative and zwitterionic charges at the two ends of pillar[5]arene channels made a big difference in water permeability (Fig. 12e). It was displayed that positive charges assisted to reduce the collective hydrogen bonding lifetime thus achieving improved water transport performance [111]. Interesting, the high-water permeability of **AAQP** enables the restoration of the water transport of cells containing function-lost AQPs, developing a new strategy for the treatment of AQP-related diseases [112] and most importantly first medical application of AWCs.

3.4.4. Pillar[5]arene poly carboxylate dimers (PAD)

Our group in collaboration with Ogoshi and Baaden groups has discovered another interesting selective water translocation mechanism along peralkyl-carboxylate-pillar[5]arenes dimers [113]. The hollow pore was adjusted to 2.8 Å by self-assembly of the twisted carboxy-phenyl moieties on pillar[5]arene backbone, which helps to block large cations and transport water selectively. To gain further insights into the water channel mechanism, the crystal structure of PAD4 was analyzed, presenting two dimeric conformations pS-pS and pR-pR along the tubular channel (Fig. 13a). The polar region (carboxylic moiety) assisted the connection with phospholipid head, the aliphatic chains enabled to insert into the lipid and the longer chains may stabilize the membrane environment to the more degree. Thanks to the simulation approach, a water wetting-dewetting process was shown along the carboxylate dimer honeycomb, followed by a slight tilt which led to the water penetration as shown in Fig. 13b.

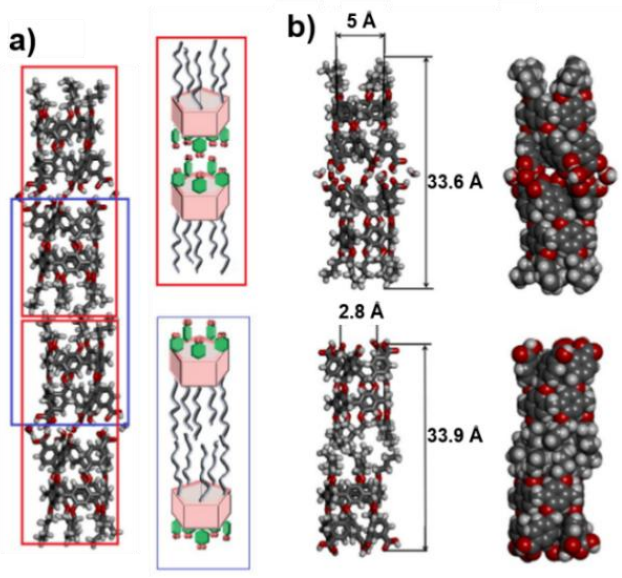

Fig. 13. (a) The crystal structure of Pillar[5]arene poly carboxylate dimers PAD4: (b) carboxylate and hydrophobic interactions of possible dimers of PAD4. Reproduced with permission from Reference [113] Copyright © 2020 WILEY-VCH GmbH.

3.4.5. Peptide-appended hybrid[4]arene (PAH[4])

The cumulative understanding of pillar arenes functional channel superstructures has provided other strategies for the fabrication of new functional species. A narrow unimolecular channel was constructed by using a pillar[4]arene scaffold by grafting eight $(Phe)_3$ chains at the two entrances[114]. MD simulation mentioned that water clusters are observed within PAH[4]-embedded bilayers. This resulted in cooperative water wire permeation supported by an energy-minimized horizontal-orientation windows mechanism. Instead of a traditional single water file within the inner PAH[4] channel cavity, water clusters were interconnected between adjacent channels on their outer surface, achieving multiple water-wire paths and paving the way toward applications for the construction of polymeric membranes with surface permeance selectivity. Although undergoing an unpredicted long itinerary, more than 10^9 water molecules/s can be transported along each channel in average.

3.5. Carbon-enriched nanochannels

Carbon-enriched materials including carbon nanotubes and graphene oxide nanostructures have attracted much attention due to their confined hydrophobic or hybrid hydrophobic/hydrophilic channels featuring important combined structural information for water translocation. Several typical examples, involving various carbon nanotubes, graphene nanopores, or nanosheets have been listed below.

3.5.1. Carbon nanotube porins

Carbon nanotubes CTNs are one-dimensional quantum nanomaterials with a tubular axial structure and extremely hydrophobic surfaces which makes it perfect as a channel alternative. It has been two decades since CTNs were proposed for studying water conduction performances by varying mechanical and physical properties [115,116, 117]. As is known, the continuous hydrogen bonding interaction between water molecules makes a big difference in the transport of water through the absolute hydrophobic environment [118], while the influence of tube length is negligible [116]. A one-dimensionally continuous water wire in a single-walled carbon nanotube has been reported by Hummer using molecular dynamics simulations and Markovian CTRW [119,120]. It was shown that five H-bonded water molecules with a distance of 2.6 Å were filled in the nanotube which has a diameter of 8.1 Å and a length of 13.4 Å. Stimulated by osmotic pressure, it was determined that 5.8 water molecules can be transported through the nanotube per nanosecond [121].

Then, Noy's group has elucidated the proton and water permeability in 0.8-nm-diameter carbon nanotube porins (CNTPs) along a one-dimensional water wire [122,123]. Enhanced proton transport can be observed in the more confined environment than that in 1.5-nm-diameter CTN porins even though the latter present bulk water in the tube, thus indicating the necessity of water confinement for improving proton transport rates. In addition, this subnanometer CNTP was able to reject chloride ions selectively and keep a good water-salt permselectivity balance at the commercial desalination membrane level [124]. From the simulated models, 12 water molecules were found to occupy the whole tube as shown in Fig. 14a, and they displayed three different dipolar states along the channel for the formation of a water wire.

To improve the biocompatibility of carbon nanotubes in the biological environment, a class of double-walled carbon nanotubes (DWCNT) was designed, it has an outer tube with hydrophilic ends (Fig.14b) to capture the free water molecules as well as protect the inner tube for achieving effective water permeation [125].

Additionally, the presence and spreading of water inside the multiwalled carbon nanotube was observed using a transmission electron microscope under the heating from 25°C to 75°C [126]. The retarded

movement of water molecules may attribute to the interaction between water and tube walls.

In total, the absolute hydrophobicity and tubular architecture of carbon nanotubes bring the prospects in the water transport for desalination and purification. However, it is not meaning the absence of its drawback, for instance, the repulsion of the rim to water molecules, the selectivity-permeability trade-off. Thus further studies and simulations on the functionalization of CTN mouth as well as the optimization of radical diameter need to be studied. The applications of carbon nanotubes for the construction of large scale membranes is more or less affected by the relative difficult production of open size pores and the generation of pore gate keepers to push water inside nanotubes

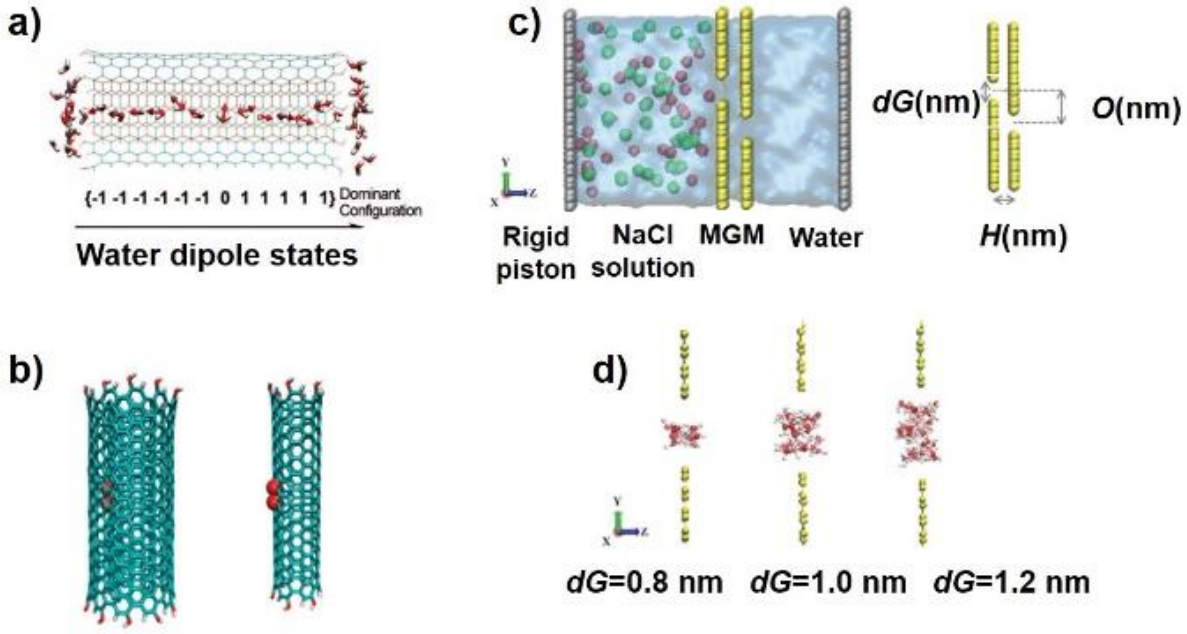

Fig. 14. (a) The water dipole states and dominant configuration of water molecules within CTNs; (b) Designed models of DWCNT and SWCNT with charged carbon atoms for water capture (in red) and end caping hydroxyl groups gate keepers. Reproduced with permission from Reference [126] Copyright © 2009 American Chemical Society; (c) The desalination model using multilayer graphene membrane (MGM) and its inner arrangement, dG is the gap width, H is the interlayer spacing, O is the offset; (d) The simulated water clusters within the gaps of MGM at different gap width. Reproduced with permission from Reference [128] Copyright © 2022 Elsevier.

3.5.2. Graphene-based 2D nanochannel

Parallel to carbon nanotube, the carbon-based graphene material, as a two-dimensional lamellar channel was proposed to be used for selective water confinement in its narrow space [127, 128]. The transport of water molecules is mainly dependent on the two-dimensional network between the stacked carboxylate/hydroxyl graphene sheets which both the nanopore size and charges are the common factors for adjusting the water flux and selectivity (Fig. 14c-14d), while the hydrogen bonding among water molecules may restrict water flux by increasing permeation energy [129–132]. Beyond this, graphene oxide and its derivatives have been used in upscaled hybrid membrane systems for water treatment [133]. Xu and coworkers reported a chitosan-modified graphene oxide membrane [134], having the hydrophilic polymer for capturing water molecules through hydrogen bonding and filtering impurities, and graphene oxide laminate as 2D channels for effective water permeation. More studies on the functionalization of graphene oxide surface and layer distance are worth to continuing for the further development of graphene oxide in the fabrication of efficient membranes for environmental applications.

3.6. Porous cage or material systems

In the past decades, multiple of porous materials have been made for water treatment [135-137], for example metal-organic frameworks, covalent organic frameworks, zeolites, and porous organic polymers. The common feature of porous systems is having Ångström level or nano-level cavities for water accommodation while excluding salts or contaminants, thus providing more possibilities for the development of porous systems in water purification. Several representative examples are listed below.

3.6.1. Tetrahedral-shaped porous organic cages

Zhao and coworkers have reported a class of tetrahedral-shaped porous organic cages (POCs) used as novel zero-dimensional nanopores for water transport and embedded in bilayer membranes and polyamide membrane desalination [138]. The transport of water molecules can be achieved through the narrow windows of POCs as shown in Fig. 15a, where they need to undergo the strongest energy barrier between two cage units (a 5-step mechanism). Self-assembling such cage molecules with a optimal density represent an important strategy to generate highly competitive membranes for desalination.

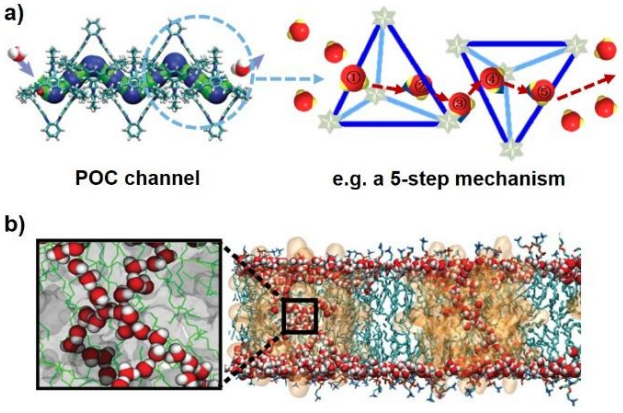

Fig. 15. (a) The transport of water and a 5-step mechanism for water transport along the POC channel; (b) The formed water chains along channels CC3 and CC19 by simulations. Reproduced with permission from Reference [138] Copyright © 2020 Springer Nature.

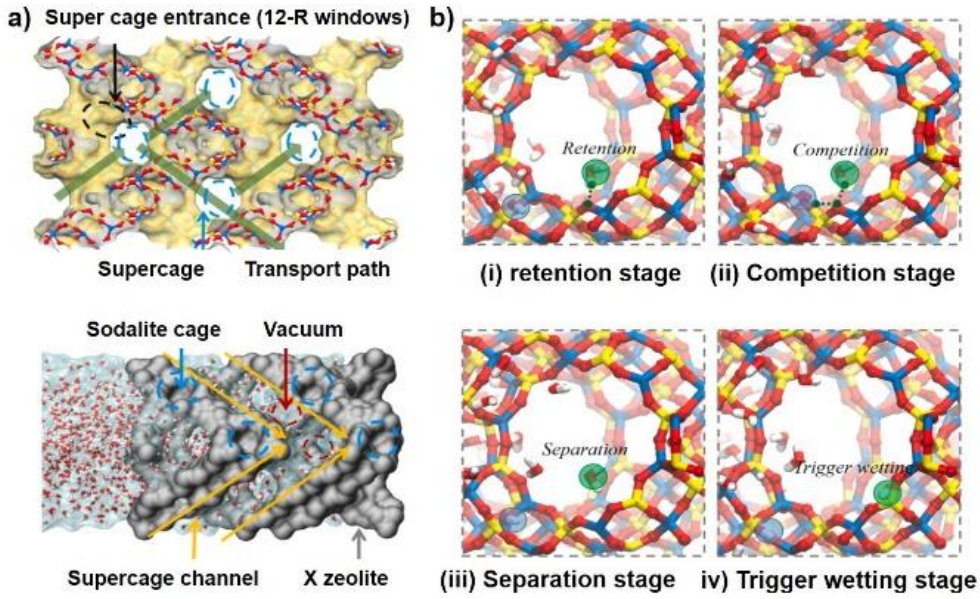

Fig. 16. (a) The structural water distribution within the 13X-zeolite; (b) The simulated dynamic wetting process of the internal zeolite pore . Reproduced with permission from Reference [139] Copyright © 2021 Elsevier.

Table 1. The possible water distribution and hydrogen bonding interaction along artificial water channels.

	Pore size (or gap width)	H-bond of Channel – Water	Water arrangement	Ref
Self-assembled channels	2.6 – 4 Å	$H_{(H2O)}$-$N_{(imidazole)}$ $O_{(H2O)}$-$HN_{(imidazole)}$ $O_{(H2O)}$-$HO_{(hydroxyl)}$ $H_{(H2O)}$-$O_{(amide)}$	Single-wires; Water clusters	[69-75]
Aromatic foldamers	2.8 – 6.5 Å	$H_{(H2O)}$-$O_{(pyridone)}$ $H_{(H2O)}$-$N_{(pyridine)}$ $H_{(H2O)}$-$O_{(ether)}$ $O_{(H2O)}$ -$H_{(amide)}$	Single-wires; Water clusters	[83-89], [91-92]
Macrocycles	5.5 – 19 Å	$H_{(H2O)}$-$O_{(amide)}$	Single-wires; Water clusters	[95-96], [98-99]
Pillar[n]arenes	1.5 – 6.5 Å	$H_{(H2O)}$-$O_{(carboxylic\ carbonyl)}$ $H_{(H2O)}$-$O_{(carboxylic\ hydroxyl\ )}$ $H_{(H2O)}$-$N_{(triazole)}$ $H_{(H2O)}$-$O_{(ether)}$	Single-wires; Water clusters	[104-114]
Organic cages	4.0 – 10.7 Å	$H_{(H2O)}$-$O_{(cage)}$ $O_{(H2O)}$-$HO_{(hydroxyl)}$ $H_{(H2O)}$-$N_{(cage)}$ or $O_{(H2O)}$-$HN_{(cage)}$	Single-wires and water clusters	[138-139]
Carbon-based nanochannels	6.8 – 29.8 Å	/	Single-wires; Water clusters	[118-128]

Benefiting from the higher hydrophilicity, channel CC19 can encapsulate more water molecules inside the cage compared to channel CC3, but meanwhile leading to higher resistance for water movement. The possible water encapsulation and hydrogen bonding interactions are depicted in Fig. 15b. Along with the simulation graph, the distribution of water in CC3 and CC9 displayed the single-file wires with a dipolar-ordered arrangement following opposite orientations along neighboring transport pathways. Again an optimal H-bonding anchoring is necessary to stabilize these clusters in multiple pore regions within the membrane.

3.6.2. Zeolite nanomaterials

The distribution and transport of water molecules in multi-porous 13X zeolite ($Na_{96}Al_{96}Si_{96}O_{384}$) was elucidated by Wang through molecular dynamics simulations (Fig. 16a) [139]. Water molecules enter the zeolite pores along the green transport pathways through the 12-R windows, and then a small amount of water can be transported into subsequent super cages due to the strong absorption behavior of channel entrance to the water, causing the sudden breakage of water clusters inside the cavity as coined a vacuum. A four-step wetting process was explained as the retention stage of the frontier water (H_{H2O}-O_{cage}), the competition stage between the frontier water and subsequent water (H_{H2O}-O_{cage}-H_{H2O}), separation stage of the frontier water and triggering wetting stage of the next water (Fig. 16b). This work may envision the further study on channel mechanism and actual utilization of nanoporous zeolite for the fabrication of upscaled membranes with *per* area permeability for water treatment.

4. Conclusion and outlook

To date, several hundreds of tailored compounds have been accounted and synthesized as selective Artificial Water channels for their potential utilization in water separation or purification. From a broad point of view, interdisciplinary research provides researchers from different fields with numerous opportunities for innovative molecular construction, no matter from overall architecture design or molecular modification, its unique structure is worthy of in-depth research and evaluation on the direction of channel functions. Noticeably, the countless reported results of artificial channels enlarge the field of molecular separations, for instance involving in the synthesis and their inclusion in bilayer and solid membranes. From the perspective of structural properties, the transport mechanism may consider the channel architecture and dimension as well as the water single-wires or cluster self-assembly and water-channel interaction of each template (Table 1). The continuous water wires or water clusters can interfere with the single channels or pores. Until now, exclusively a small amount of clear examples have been elucidated comprehensively for practical utilization but important useful information is gained by exploiting the simulation approach at Ångström-scale observation. Thus this is still broad room for continuous efforts in the interpretation of artificial water channels.

In this review, artificial water channels currently reported are listed and classified into organic cages, macrocycles, carbon-based nanopores, aromatic foldamers, pillar[n]arenes, and self-assembled channels. The pore-forming property of these compounds offers a path to accommodate water molecules along the channel axle, giving rise to equal or over AQP-level water translocation. In particular, water distribution and orientation based on hydrogen bonding interaction is the key point when we explore important behaviors of the transport mechanism of each channel. Having sufficient microscale analysis, the development of an artificial channel-inserted solid membrane can be envisioned for environmental applications. In this case, additional precautions need to be necessarily considered, such as the reliable evaluation of transport performance and observation of water arrangement in real membrane systems, the optimization of artificial channel-embedded membranes under harsh conditions etc.

Acknowledgements

This work was supported by the project “Evolution” funded by European Union – NextgenerationEU and Romanian Government, under National Recovery and Resilience Plan for Romania, contract no.760033/23.05.2023/23.05.2023, cod PNRR-C9-I8-CF16, through the Romanian Ministry of Research, Innovation and Digitalization, within Component 9, Investment I8”. Dan-Dan Su appreciates receiving a scholarship (CSC number: 201906790018) from China Scholarship Council as support at University of Montpellier, France.

REFERENCES

[1] C. G. Salzmann, P. G. Radaelli, A. Hallbrucker, E. Mayer, J. L. Finney, The preparation and structures of hydrogen ordered phases of ice, Geophys. Res. Lett. 31 (2004) 787, https://doi.org/10.1126/science.1123896.

[2] G. Kerch, Role of changes in state of bound water and tissue stiffness in development of age-related diseases, Polymers. 12 (2020) 1362, https://doi.org/10.3390/polym12061362.

[3] G. Kerch, Distribution of tightly and loosely bound water in biological macromolecules and age-related diseases, Int. J. Biol. Macromol. 118 (2018) 1310–1318, https://doi.org/10.1016/j.ijbiomac.2018.06.187.

[4] K.R. Heys, M.G. Friedrich, R.J.W. Truscott, Free and bound water in normal and cataractous human lenses, Invest. Ophth. Vis. Sci. 49 (2008) 1991–1997, https://doi.org/10.1167/iovs.07-1151.

[5] G.M. Smith, R.S. Alexander, D.W. Christianson, B.M. McKeever, G.S. Ponticello, J.P. Springer, W.C. Randall, J.J. Baldwin, C.N. Habecker, Positions of His-64 and a bound water in human carbonic anhydrase II upon binding three structurally related inhibitors, Protein Sci. 3 (1994) 118–125, https://doi.org/10.1002/pro.5560030115.

[6] W. E. C. Harries, D. Akhavan, L. J. W. Miercke, S. Khademi, R. M. Stroud, The channel architecture of aquaporin 0 at a 2.2-Å resolution, Proc. Natl. Acad. Sci. 101 (2004) 14045–14050, https://doi.org/10.1073/pnas.0405274101.

[7] Tamtaji, M. Behnam, M.A. Pourattar, H. Jafarpour, Z. Asemi, Aquaporin 4: A key player in Parkinson's disease, J. Cell. Physiol. 234 (2019) 21471–21478, https://doi.org/10.1002/jcp.28871.

[8] E. Beitz, P. Agre, Regulation of aquaporin-2 trafficking, Handb. Exp. Pharmacol. 190 (2009) Aquaporins pp 133-150, https://link.springer.com/chapter/10.1007/978-3-540-79885-9_6.

[9] J.D. Ho, R. Yeh, A. Sandstrom, I. Chorny, W.E.C. Harries, R.A. Robbins L.J.W. Miercke, R.M. Stroud, Crystal structure of human aquaporin 4 at 1.8 Å and its mechanism of conductance, Proc. Natl. Acad. Sci. 106 (2009) 7437–7442, https://doi.org/10.1073/pnas.090272510.

[10] Y. Song, N. Sonawane, A.S. Verkman, Localization of aquaporin-5 in sweat glands and functional analysis using knockout mice, J. Physiol. 541 (2002) 561–568, https://doi.org/10.1113/jphysiol.2001.020180.

[11] P. Agre, Molecular physiology of water transport: aquaporin nomenclature workshop. Mammalian aquaporins, Biol. Cell 89 (1997) 255–257, https://doi.org/10.1016/S0248-4900(97)83377-1.

[12] L.S. King, M. Choi, P.C. Fernandez, J.-P. Cartron, P. Agre, Defective urinary concentrating ability due to a complete deficiency of aquaporin-1, N. Engl. J. Med. 345 (2001) 175-179, https://doi.org/10.1056/NEJM200107193450304.

[13] S.W. de Maré, R. Venskutonytė, S. Eltschkner, B.L.d. Groot, K. Lindkvist-Petersson, Structural basis for glycerol efflux and selectivity of human aquaporin 7, Structure 28 (2020) 215-222, https://doi.org/10.1016/j.str.2019.11.011.

[14] D.C. Soler, X. Bai, L. Ortega, T. Pethukova, S.T. Nedorost, D.L. Popkin, K.D. Cooper, T.S. McCormick, The key role of aquaporin 3 and aquaporin 10 in the pathogenesis of pompholyx, Med. Hypotheses 84 (2015) 498–503, https://doi.org/10.1016/j.mehy.2015.02.006.

[15] J. Badaut, L. Regli, Distribution and possible roles of aquaporin 9 in the brain, Neurosci. 129 (2004) 971–981, https://doi.org/10.1016/j.neuroscience.2004.06.035.

[16] R. Sougrat, M. Morand, C. Gondran, P. Barré, R. Gobin, F. Bonté,

M. Dumas, J.-M. Verbavatz, Functional expression of AQP3 in human skin epidermis and reconstructed epidermis, J. Invest. Dermatol. 118 (2002) 678–685, https://doi.org/10.1046/j.1523-1747.2002.01710.x.

[17] M. Zelenina, A.A. Bondar, S. Zelenin, A. Aperia, Nickel and extracellular acidification inhibit the water permeability of human aquaporin-3 in lung epithelial cells, J. Biol. Chem. 278 (2003) 30037–30043, https://doi.org/10.1074/jbc.M302206200.

[18] R.M. Bill, K. Hedfalk, Aquaporins-expression, purification and characterization, Biochim. Biophys. Acta Biomembr. 1863 (2021) 183650, https://doi.org/10.1016/j.bbamem.2021.183650.

[19] J.A. Bornhorst, J.J. Falke, Purification of proteins using polyhistidine affinity tags, Meth. Enzymol. 326 (2000) 245–254, https://doi.org/10.1016/S0076-6879(00)26058-8.

[20] G. Calamita, W.R. Bishai, G.M. Preston, W.B. Guggino, P. Agre, Molecular cloning and characterization of AqpZ, a water channel from Escherichia coli, J. Biol. Chem. 270 (1995) 29063–29066, https://doi.org/10.1074/jbc.270.49.29063.

[21] Y. Zhao, X. Li, J. Wei, J. Torres, A.G. Fane, R. Wang, C.Y. Tang, Optimization of aquaporin loading for performance enhancement of aquaporin-based biomimetic thin-film composite membranes, Membranes 12 (2022) 1–14, https://doi.org/10.3390/membranes12010032.

[22] D.-D. Su, M. Barboiu, Artificial water channels-progress innovations and prospects, CCS Chem. 5, (2023) 279–291, https://doi.org/10.31635/cschem.022.202202353.

[23] L.-B. Huang, M. Di Vincenzo, Y. Li, M. Barboiu, Artificial water channels: towards biomimetic membranes for desalination, Chem. -Eur. J. 27 (2021) 2224–2239, https://doi.org/10.1002/chem.202003470.

[24] W. Song, M. Kumar, Artificial water channels: toward and beyond desalination, Curr. Opin. Chem. Eng. 25 (2019) 9–17, https://doi.org/10.1016/j.coche.2019.06.007.

[25] M. Baaden, M. Barboiu, R.M. Bill, C.-L. Chen, J. Davis, M. Di Vincenzo, V. Freger, M. Fröba, P.A. Gale, B. Gong, C. Hélix-Nielsen, R. Hickey, B. Hinds, J.-L. Hou, G. Hummer, M. Kumar, Y.-M. Legrand, M. Lokesh, B. Mi, S. Murail, P. Pohl, M. Sansom, Q. Song, W. Song, S. Törnroth-Horsefield, H. Vashisth, M. Vögele, Biomimetic water channels: general discussion, Faraday Discuss. 209 (2018) 205–229, https://doi.org/10.1039/C8FD90020E.

[26] B. Gong, Artificial water channels: inspiration, progress, and challenges, Faraday Discuss. 209 (2018) 415–427, https://doi.org/10.1039/C8FD00132D.

[27] M. Barboiu, A. Gilles, From natural to bioassisted and biomimetic artificial water channel systems, Acc. Chem. Res. 46 (2013) 2814–2823, https://doi.org/10.1021/ar400025e.

[28] M. Fasano, T. Humplik, A. Bevilacqua, M. Tsapatsis, E. Chiavazzo, E.N. Wang, P. Asinari, Interplay between hydrophilicity and surface barriers on water transport in zeolite membranes, Nat. Commun. 7 (2016) 12762, https://doi.org/10.1038/ncomms12762.

[29] D. Strilets, S. Cerneaux, M. Barboiu, Enhanced desalination polyamide membranes incorporating pillar[5]arene through in-situ aggregation-interfacial polymerization-isAGRIP, ChemPlusChem 86 (2021) 1602–1607, https://doi.org/10.1002/cplu.202100473.

[30] Y.J. Lim, K. Goh, R. Wang, The coming of age of water channels for separation membranes: from biological to biomimetic to synthetic, Chem. Soc. Rev. 51 (2022) 4537–4582, https://doi.org/10.1039/D1CS01061A.

[31] G. Goel, C. Hélix-Nielsen, H.M. Upadhyaya, S. Goel, A bibliometric study on biomimetic and bioinspired membranes for water filtration, *npj* Clean Water 4 (2021) e108, https://doi.org/10.1038/s41545-021-00131-4.

[32] J. Zhang, C. Chen, J. Pan, L. Zhang, L. Liang, Z. Kong, X. Wang, W. Zhang, J.-W. Shen, Atomistic insights into the separation mechanism of multilayer graphene membranes for water desalination, Phys. Chem. Chem. Phys. 22 (2020) 7224–7233, https://doi.org/10.1039/D0CP00071J.

[33] B. Mi, S. Zheng, Q. Tu, 2D graphene oxide channel for water transport, Faraday discuss. 209 (2018) 329–340, https://doi.org/10.1039/C8FD00026C.

[34] Q. Xie, M.A. Alibakhshi, S. Jiao, Z. Xu, M. Hempel, J. Kong, H.G. Park, C. Duan, Fast water transport in graphene nanofluidic channels, Nat. Nanotechnol. 13 (2018) 238–245, https://doi.org/10.1038/s41565-017-0031-9.

[35] T. Humplik, J. Lee, S. O'Hern, T. Laoui, R. Karnik, E.N. Wang, Enhance dwater transport and salt rejection through hydrophobic zeolite pores, Nanotechnology 28 (2017) 505703, https://doi.org/10.1088/1361-6528/aa9773.

[36] Y.-X. Shen, P.O. Saboe, I.T. Sines, M. Erbakan, M. Kumar, Biomimetic membranes: A review, J. Membr. Sci. 454 (2014) 359–381, https://doi.org/10.1016/j.memsci.2013.12.019.

[37] W. Si, L. Chen, X.-B. Hu, G. Tang, Z. Chen, J.-L. Hou, Z.-T. Li, Selective artificial transmembrane channels for protons by formation of water wires, Angew. Chem. Int. Ed. 50 (2011) 12564–12568, https://doi.org/10.1002/anie.201106857.

[38] T.E. Decoursey, Voltage-gated proton channels and other proton transfer pathways, Physiol. Rev. 83 (2003) 475–579, https://doi.org/10.1152/physrev.00028.2002.

[39] M.G. Preston, Carroll, Piazza, Tiziana, B.W. Guggino, P. Agre, Appearance of water channels in xenopus oocytes expressing red cell CHIP28 protein, Science 256 (1992) 385–387, https://doi.org/10.1126/science.256.5055.385.

[40] P. Agre, The Aquaporin Water Channels, Proc. Am. Thorac. 3 (2006) 5–13, https://doi.org/10.1513/pats.200510-109JH.

[41] A. Adeoye, A. Odugbemi, T. Ajewole, Structure and function of aquaporins: the membrane water channel proteins, Biointerface Res. Appl. Chem. 12 (2021) 690–705, https://doi.org/10.33263/BRIAC121.690705.

[42] E. Tajkhorshid, P. Nollert, M. Jensen, L.J.W. Miercke, J. O'Connell, R.M. Stroud, K. Schulten, Control of the selectivity of the aquaporin water channel family by global orientational tuning, Science 296 (2002) 525–530, https://doi.org/10.1126/science.1067778.

[43] B.L.d. Groot, H. Grubmuller, Water permeation across biological membranes: mechanism and dynamics of aquaporin-1 and GlpF, Science 294 (2001) 2353–2357, https://doi.org/10.1126/science.1066115.

[44] K. Murata, K. Mitsuoka, T. Hirai, T. Walz, P. Agre, J.B. Heymann, A. Engel, Y. Fujiyoshi, Structural determinants of water permeation through aquaporin-1, Nature 407 (2000) 599–605, https://doi.org/10.1038/35036519.

[45] L.M. Zeidel, S. Nielsen, L.B. Smith, V.S. Ambudkar, B.A. Maunsbach, P. Agre, Ultrastructure, pharmacologic inhibition, and transport selectivity of aquaporin CHIP in proteoliposomes, Biochem. 33 (1994) 1606–1615, https://doi.org/10.1021/bi00172a042.

[46] T. Walz, B.L. Smith, M.L. Zeidel, A. Engel, P. Agre, Biologically active two-dimensional crystals of aquaporin CHIP, J. Biol. Chem. 269 (1994) 1583–1586, https://doi.org/10.1016/S0021-9258(17)42062-X.

[47] J.S. Hub, B.L.d. Groot, Mechanism of selectivity in aquaporins and aquaglyceroporins, Proc. Natl. Acad. Sci. 105 (2008) 1198–1203, https://doi.org/10.1073/pnas.0707662104.

[48] H. Sui, B.-G. Han, J.K. Lee, P. Walian, B.K. Jap, Structural basis of water-specific transport through the AQP1 water channel, Nature 414 (2001) 872-878, https://doi.org/10.1038/414872a.

[49] X. Li, R. Wang, C. Tang, A. Vararattanavech, Y. Zhao, J. Torres, T. Fane, Preparation of supported lipid membranes for aquaporin Z incorporation, Colloids Surf. 94 (2012) 333–340, https://doi.org/10.1016/j.colsurfb.2012.02.013.

[50] P.S. Zhong, T.-S. Chung, K. Jeyaseelan, A. Armugam, Aquaporin-embedded biomimetic membranes for nanofiltration, J. Membr. Sci. 407-408 (2012) 27–33, https://doi.org/10.1016/j.memsci.2012.03.033.

[51] Y. Li, S. Qi, M. Tian, W. Widjajanti, R. Wang, Fabrication of aquaporin-based biomimetic membrane for seawater desalination, Desalination 467 (2019) 103–112, https://doi.org/10.1016/j.desal.2019.06.005.

[52] M. Kumar, M. Grzelakowski, J. Zilles, M. Clark, W. Meier, Highly permeable polymeric membranes based on the incorporation of the functional water channel protein Aquaporin Z, Proc. Natl. Acad. Sci. 104 (2007) 20719–20724, https://doi.org/10.1073/pnas.0708762104.

[53] M. Kumar, J.E.O. Habel, Y.-X. Shen, W.P. Meier, T. Walz, High-density reconstitution of functional water channels into vesicular and planar block copolymer membranes, J. Am. Chem. Soc. 134 (2012) 18631–18637, https://doi.org/10.1021/ja304721r.

[54] Y.-M. Tu, W. Song, T. Ren, Y.-X. Shen, R. Chowdhury, P. Rajapaksha, T. E. Culp, L. Samineni, C. Lang, A. Thokkadam, D. Carson, Y. Dai, A. Mukthar, M. Zhang, A. Parshin, J.N. Sloand, S.H. Medina, M. Grzelakowski,D. Bhattacharya, W.A. Phillip, E.D. Gomez, R.J. Hickey, Y.Wei, M. Kumar, Rapid fabrication of precise high-throughput filters fro m membrane protein nanosheets, Nat. Mater. 19 (2020) 347–354, https://doi.org/10.1038/s41563-019-0577-z.

[55] W. Song, Y.-M. Tu, H. Oh, L. Samineni, M. Kumar, Hierarchical optimization of high-performance biomimetic and bioinspired membrane, Langmuir. 35 (2019) 589–607, https://doi.org/10.1021/acs.langmuir.8b03655.

[56] C.Y. Tang, Y. Zhao, R. Wang, C. Hélix-Nielsen, A.G. Fane, Desalination by biomimetic aquaporin membranes: Review of status and prospects, Desalination 308 (2013) 34–40, https://doi.org/10.1016/j.desal.2012.07.007.

[57] B. Roux, Computational studies of the gramicidin channel, Acc. Chem. Res. 35 (2002) 366–375, https://doi.org/10.1021/ar010028v.

[58] R. Pomès, B. Roux, Structure and dynamics of a proton wire: a theoretical study of H+ translocation along the single-file water chain in the gramicidin A channel, Biophys. J. 71 (1996) 19–39, https://www.cell.com/biophysj/pdf/S0006-3495(96)79211-1.pdf.

[59] Mark L. Brewer, Udo W. Schmitt, Gregory A. Voth, The formation and dynamics of proton wires in channel environments, Biophys. J. 80 (2001) 1691–1702, https://www.cell.com/biophysj/pdf/S0006-3495(01)76140-1.pdf.

[60] L.H. Pinto, G.R. Dieckmann, C.S. Gandhi, C.G. Papworth, J. Braman, M. A. Shaughnessy, J.D. Lear, R.A. Lamb, W.F. DeGrado, A functionally defined model for the M2 proton channel of influenza A virus suggests a mechanism for its ion selectivity, Proc. Natl. Acad. Sci. 94 (1997) 11301–11306, https://doi.org/10.1073/pnas.94.21.11301.

[61] M.S.P. Sansom, I.D. Kerr, G. R. Smith, H. S. Son, The influenza A virus M2 channel: a molecular modeling and simulation study, Virology 233 (1997) 163–173, https://doi.org/10.1006/viro.1997.8578.

[62] V. Vijayvergiya, R. Wilson, A. Chorak, P.F. Gao, T.A. Cross, D.D. Busath, Proton conductance of influenza virus M2 protein in planar lipid bilayers, Biophys. J. 87 (2004) 1697–1704, https://www.cell.com/biophysj/pdf/S0006-3495(04)73650-4.pdf.

[63] S. Phongphanphanee, T. Rungrotmongkol, N. Yoshida, S. Hannongbua, F. Hirata, Proton transport through the influenza A M2 channel: three-dimensional reference interaction site model study, J. Am. Chem. Soc. 132 (2010) 9782–9788, https://doi.org/10.1021/ja1027293.

[64] J.R. Schnell, J.J. Chou, Structure and mechanism of the M2 proton channel of influenza A virus, Nature 451 (2008) 591–595, https://doi.org/10.1038/nature06531.

[65] D.A. Doyle, J.M. Cabral, R.A. Pfuetzner, A. Kuo, J.M. Gulbis, S.L. Cohen, B.T. Chait, R. MacKinnon, The structure of the potassium channel: molecular basis of K+ conduction and selectivity, Science 280 (1998) 69–77, https://doi.org/10.1126/science.280.5360.69.

[66] Z. Ganim, A. Tokmakoff, A. Vaziri, Vibrational excitons in ionophores: Experimental probes for quantum coherence-assisted ion transport and selectivity in ion channels, New J. Phys. 13 (2011) 113030, https://doi.org/10.1088/1367-2630/13/11/113030.

[67] J.H. Morais-Cabral, Y. Zhou, R. MacKinnon, Energetic optimization of ion conduction rate by the K+ selectivity filter, Nature 414 (2001) 37–42, https://doi.org/10.1038/35102000.

[68] V. Percec, A. E. Dulcey, V. S. K. Balagurusamy, Y. Miura, J. Smidrkal, M. Peterca, S. Nummelin, U. Edlund, S. D. Hudson, P. A. Heiney, H. Duan, S. N. Magonov, S. A. Vinogradov, Self-assembly of amphiphilic dendritic dipeptides into helical pores, Nature 430 (2004) 764–768, https://doi.org/10.1038/nature02770.

[69] E. Licsandru, I. Kocsis, Y.-X. Shen, S. Murail, Y.-M. Legrand, A. van der Lee, D. Tsai, M. Baaden, M. Kumar, M. Barboiu, Salt-excluding artificial water channels exhibiting enhanced dipolar water and proton translocation, J. Am. Chem. Soc. 138 (2016) 5403–5409, https://doi.org/10.1021/jacs.6b01811.

[70] Y. Le Duc, M. Michau, A. Gilles, V. Gence, Y.-M. Legrand, A. van der Lee, S. Tingry, M. Barboiu, Imidazole-quartet water and proton dipolar channels, Angew. Chem. Int. Ed. 50 (2011) 11366–11372, https://doi.org/10.1002/ange.201103312.

[71] L.-B. Huang, M. Di Vincenzo, M.G. Ahunbay, A. van der Lee, D. Cot, S. Cerneaux, G. Maurin, M. Barboiu, Bilayer versus polymeric artificial water channel membranes: structural determinants for enhanced filtration performances, J. Am. Chem. Soc. 143 (2021) 14386–14393, https://doi.org/10.1021/jacs.1c07425.

[72] L.-B. Huang, A. Hardiagon, I. Kocsis, C.-A. Jegu, M. Deleanu, A. Gilles, A. van der Lee, F. Sterpone, M. Baaden, M. Barboiu, Hydroxy channels–adaptive pathways for selective water cluster permeation, J. Am. Chem. Soc. 143 (2021) 4224–4233, https://doi.org/10.1021/jacs.0c11952.

[73] A. Ghahari, H. Raissi, F. Farzad, S. Pasban, Design of a hydroxy channel based on the selectivity of water permeation via ions exclusion, *npj* Clean Water 6 (2023) 3, https://doi.org/10.1038/s41545-022-00210-0.

[74] D. Mondal, B.R. Dandekar, M. ahmad, A. Mondal, J. Mondal, P. Talukdar, Selective and rapid water transportation across a self-assembled peptide-diol channel via the formation of a dual water array, Chem. Sci. 13 (2022) 9614–9623, https://doi.org/10.1039/D2SC01737G.

[75] D.G. Dumitrescu, J. Rull-Barull, A.R. Martin, N. Masquelez, M. Polentarutti, A. Heroux, N. Demitri, G. Bais, I.-T. Moraru, R. Poteau, M. Amblard, A. Krajnc, G. Mali, Y.-M. Legrand, A. van der Lee, B. Legrand, The unexpected helical supramolecular assembly of a simple achiral acetamide tecton generates selective water channels, Chem. -Eur. J. 28(2022) e202200383, https://doi.org/10.1002/chem.202200383.

[76] S.-P. Zheng, Y.-H. Li, J.-J. Jiang, A. van der Lee, D. Dumitrescu, M. Barboiu, Self-assembled columnar triazole quartets: an example of synergistic hydrogen-bonding/anion-π interactions, Angew. Chem. Int. Ed. 131 (2019) 12165-12170, https://doi.org/10.1002/ange.201904808.

[77] M. Barboiu, Y. Le Duc, A. Gilles, P.-A. Cazade, M. Michau, Y. Marie Legrand, A. van der Lee, B. Coasne, P. Parvizi, J. Post, T. Fyles, An artificial primitive mimic of the Gramicidin-A channel, Nat. Commun. 5 (2014) 4142, https://doi.org/10.1038/ncomms5142.

[78] J. Zhu, R.D. Parra, H. Zeng, E. Skrzypczak-Jankun, X.C. Zeng, B. Gong, A new class of folding oligomers: Crescent oligoamides, J. Am. Chem. Soc. 122 (2000) 4219–4220, https://doi.org/10.1021/ja994433h.

[79] V. Berl, I. Huc, R.G. Khoury, Krische Michael J., J.-M. Lehn, Interconversion of single and double helices formed from synthetic molecular strands, Nature 407 (2000) 720–723, https://doi.org/10.1038/35037545.

[80] H. Zhao, W.Q. Ong, F. Zhou, X. Fang, X. Chen, S.F.Y. Li, H. Su, N.-J. Cho, H. Zeng, Chiral crystallization of aromatic helical foldamers via complementarities in shape and end functionalities, Chem. Sci. 3 (2012) 2042, https://doi.org/10.1039/C2SC20219K.

[81] H. Zhao, W.Q. Ong, X. Fang, F. Zhou, M.N. Hii, S.F.Y. Li, H. Su, H. Zeng, Synthesis, structural investigation and computational modelling of water-binding aquafoldamers, Org. Biomol. Chem. 10 (2012) 1172–1180, https://doi.org/10.1039/C1OB06609A.

[82] Y. Huo, H. Zeng, "Sticky"-ends-guided creation of functional hollow nanopores for guest encapsulation and water transport, Acc. Chem. Res. 49 (2016) 922–930, https://doi.org/10.1021/acs.accounts.6b00051.

[83] W.Q. Ong, H. Zhao, Z. Du, J.Z.Y. Yeh, C. Ren, L.Z.W. Tan, K. Zhang, H. Zeng, Computational prediction and experimental verification of pyridine-based helical oligoamides containing four repeating units per helical turn, Chem. Commun. 47 (2011) 6416–6418, https://doi.org/10.1039/C1CC115 32D.

[84] H. Zhao, S. Sheng, Y. Hong, H. Zeng, Proton gradient-induced water transport mediated by water wires inside narrow aquapores of aquafoldamer molecules, J. Am. Chem. Soc. 136 (2014) 14270–14276, https://doi.org/10.1021/ja5077537.

[85] T.W. Bell, H. Jousselin, Self-assembly of a double-helical complex of sodium, Nature 367 (1994) 441–444, https://doi.org/10.1038/367441a0.

[86] J. Shen, R. Ye, A. Romanies, A. Roy, F. Chen, C. Ren, Z. Liu, H. Zeng, Aquafoldmer-based aquaporin-like synthetic water channel, J. Am. Chem. Soc. 142 (2020) 10050–10058, https://doi.org/10.1021/jacs.0c02013.

[87] J. Shen, J. Fan, R. Ye, N. Li, Y. Mu, H. Zeng, Polypyridine-based

helical amide foldamer channels: rapid transport of water and protonswith high ion rejection, Angew. Chem. Int. Ed. 59 (2020) 13328–13334,https://doi.org/10.1002/anie.202003512.

[88] W.Q. Ong, H. Zhao, X. Fang, S. Woen, F. Zhou, W. Yap, H. Su, S.F.Y. Li, H. Zeng, Encapsulation of conventional and unconventional water dimers by water-binding foldamers, Org. Lett. 13 (2011) 3194–3197, https://doi.org/10.1021/ol2011083.

[89] J. Shen, R. Ye, Z. Liu, H. Zeng, Hybrid Pyridine-Pyridone Foldamer Channels as M2-Like Artificial Proton Channels, Angew. Chem. Int. Ed. 134 (2022) 28, https://doi.org/10.1002/ange.202200259.

[90] T. Yan, S. Liu, J. Xu, H. Sun, S. Yu, J. Liu, Unimolecular helix-based transmembrane nanochannel with a smallest luminal cavity of 1 å expressing high proton selectivity and transport activity, Nano Lett. 21 (2021) 10462–10468, https://doi.org/10.1021/acs.nanolett.1c03858.

[91] Roy, J. Shen, H. Joshi, W. Song, Y.-M. Tu, R. Chowdhury, R. Ye, N. Li, C. Ren, M. Kumar, A. Aksimentiev, H. Zeng, Foldamer-based ultrapermeable and highly selective artificial water channels that exclude protons, Nat. Nanotechnol. 16 (2021) 911–917, https://doi.org/10.1038/s41565-021-00915-2.

[92] J. Shen, A. Roy, H. Joshi, L. Samineni, R. Ye, Y.-M. Tu, W. Song, M. Skiles, M. Kumar, A. Aksimentiev, H. Zeng, Fluorofoldamer-based salt- and proton-rejecting artificial water channels for ultrafast water transport, Nano Lett. 22 (2022) 4831–4838, https://doi.org/10.1021/acs.nanolett.2c01137.

[93] M.R. Ghadiri, R.J. Granja, A.R. Milligan, E.D. McRee, N. Khazanovich, Self-assembling organic nanotubes based on a cyclic peptide architecture, Nature 366 (1993) 324–327, https://doi.org/10.1038/366324a0.

[94] C. Dutta, P. Krishnamurthy, D. Su, S. H. Yoo, G. W. Collie, M. Pasco, J. K. Marzinek, P. J. Bond, C. Verma, A. Grélard, A. Loquet, J. Li, M. Luo, M. Barboiu, G. Guichard, R. M. Kini, P. P. Kumar, Nature-inspired synthetic oligourea foldamer channels allow water transport with high salt rejection, Chem. 9 (2023) 1-18, https://doi.org/10.1016/j.chempr.2023.04.007.

[95] X. Zhou, G. Liu, K. Yamato, Y. Shen, R. Cheng, X. Wei, W. Bai, Y. Gao, H. Li, Y. Liu, F. Liu, D.M. Czajkowsky, J. Wang, M.J. Dabney, Z. Cai, J. Hu, F.V. Bright, L. He, X.C. Zeng, Z. Shao, B. Gong, Self-assembling subnanometer pores with unusual mass-transport properties, Nat. Commun. 3 (2012) 949, https://doi.org/10.1038/ncomms1949.

[96] Y. Shen, F. Fei, Y. Zhong, C. Fan, J. Sun, J. Hu, B. Gong, D.M. Czajkowsky, Z. Shao, Controlling Water Flow through a Synthetic Nanopore with Permeable Cations, ACS Cent. Sci. 7 (2021) 2092–2098, https://doi.org/10.1021/acscentsci.1c01218.

[97] H.-Y. Chang, K.-Y. Wu, W.-C. Chen, J.-T. Weng, C.-Y. Chen, A. Raj, H.-O. Hamaguchi, W.-T. Chuang, X. Wang, C.-L. Wang, Water-induced self-assembly of amphiphilic discotic molecules for adaptive artificial water channels, ACS nano 15 (2021) 14885–14890, https://doi.org/10.1021/acsnano.1c04994.

[98] Y. Itoh, S. Chen, R. Hirahara, T. Konda, T. Aoki, T. Ueda, I. Shimada, J.J. Cannon, C. Shao, J. Shiomi, K.V. Tabata, H. Noji, K. Sato, T. Aida, Ultrafast water permeation through nanochannels with a densely fluorous interior surface, Science 376 (2022) 738–743, https://doi.org/10.1126/science.abd0966.

[99] X. Li, K. Yang, J. Su, H. Guo, Water transport through a transmembrane channel formed by arylene ethynylene macrocycles, RSC Adv. 4 (2014) 3245–3252, https://doi.org/10.1039/C3RA43545H.

[100] S. Yuan, G. Zhang, J. Zheng, P. Jin, J. Zhu, J. Yang, S. Liu, P. van Puyvelde, B. van der Bruggen, Tuning intermolecular pores of resorcin [4] arene-based membranes for enhanced nanofiltration performance, J. Membr. Sci. 610 (2020) 118282, https://doi.org/10.1016/j.memsci.2020.118282.

[101]T. Ogoshi, S. Kanai, S. Fujinami, T.-A. Yamagishi, Y. Nakamoto, para-Bridged symmetrical pillar[5]arenes: their lewis acid catalyzed synthesis and host-guest property, J. Am. Chem. Soc. 130 (2008) 5022–5023, https://doi.org/10.1021/ja711260m.

[102]T. Ogoshi, K. Umeda, T.-A. Yamagishi, Y. Nakamoto, Through-space π-delocalized Pillar[5]arene, Chem. Commun. (2009) 4874–4876, https://doi.org/10.1039/B907894K.

[103]T. Ogoshi, K. Kitajima, T. Aoki, S. Fujinami, T.-A. Yamagishi, Y. Nakamoto, Synthesis and conformational characteristics of alkyl-substituted pillar [5] arenes, J. Org. Chem. 75 (2010) 3268–3273, https://doi.org/10.1021/jo100273n.

[104]W. Si, X.-B. Hu, X.-H. Liu, R. Fan, Z. Chen, L. Weng, J.-L. Hou, Self-assembly and proton conductance of organic nanotubes from pillar[5] arenes, Tetrahedron Lett. 52 (2011) 2484–2487, https://doi.org/10.1016/j.tetlet.2011.03.019.

[105]X.-B. Hu, Z. Chen, G. Tang, J.-L. Hou, Z.-T. Li, Single-molecular artificial transmembrane water channels, J. Am. Chem. Soc. 134 (2012) 8384–8387, https://doi.org/10.1021/ja302292c.

[106]L. Chen, W. Si, L. Zhang, G. Tang, Z. T. Li, J. L. Hou, Chiral selective transmembrane transport of amino acids through artificial channels, J. Am. Chem. Soc. 135, (2013), 2152-2155, https://doi.org/10.1021/ja312704e.

[107]Y.-X. Shen, W. Song, D.R. Barden, T. Ren, C. Lang, H. Feroz, C.B. Henderson, P.O. Saboe, D. Tsai, H. Yan, P.J. Butler, G.C. Bazan, W.A. Phillip, R.J. Hickey, P.S. Cremer, H. Vashisth, M. Kumar, Achieving high permeability and enhanced selectivity for Ångström-scale separations using artificial water channel membranes, Nat. Commun. 9 (2018) 2294, https://doi.org/10.1038/s41467-018-04604-y.

[108]Q. Li, X. Li, L. Ning, C.-H. Tan, Y. Mu, R. Wang, Hyperfast water transport through biomimetic nanochannels from peptide-attached (pR)-pillar [5] arene, Small 15 (2019) e1804678, https://doi.org/10.1002/smll.201804678.

[109]Y.J. Lim, G.S. Lai, Y. Zhao, Y. Ma, J. Torres, R. Wang, A scalable method to fabricate high-performance biomimetic membranes for seawater desalination: Incorporating pillar[5]arene water nanochannels into the polyamide selective layer, J. Membr. Sci. 661 (2022) 120957, https://doi.org/10.1016/j.memsci.2022.120957.

[110]Z.-J. Yan, D. Wang, Z. Ye, T. Fan, G. Wu, L. Deng, L. Yang, B. Li, J. Liu, T. Ma, C. Dong, Z.-T. Li, L. Xiao, Y. Wang, W. Wang, J.-L. Hou, Artificial aquaporin that restores wound healing of impaired cells, J. Am. Chem. Soc. 142 (2020) 15638–15643, https://doi.org/10.1021/jacs.0c00601.

[111] Horner, C. Siligan, A. Cornean, P. Pohl, Positively charged residues at the channel mouth boost single-file water flow, Faraday Discuss. 209 (2018) 55-65, https://doi.org/10.1039/C8FD00050F.

[112] Q. Xiao, T. Fan, Y. Wang, Z.-T. Li, J.-L. Hou, Y. Wang, Artificial water channel that couples with cell protrusion formation, CCS Chem. 5 (2023) 1745-1752, https://doi/org/10.31635/ccschem.023.202302975.

[113] D. Strilets, S. Fa, A. Hardiagon, M. Baaden, T. Ogoshi, M. Barboiu, Biomimetic approach for highly selective artificial water channels based on tubular pillar [5] arene dimers, Angew. Chem. Int. Ed. 59 (2020) 23213–23219, https://doi.org/10.1002/anie.202009219.

[114] W. Song, H. Joshi, R. Chowdhury, J.S. Najem, Y.-X. Shen, C. Lang, C. B. Henderson, Y.-M. Tu, M. Farell, M.E. Pitz, C.D. Maranas, P.S. Cremer, R.J. Hickey, S.A. Sarles, J.-L. Hou, A. Aksimentiev, M. Kumar, Artificialwater channels enable fast and selective water permeation through water-wire networks, Nat. Nanotechnol. 15 (2020) 73–79, https://doi.org/10.1038/s41565-019-0586-8.

[115] Y. Hou, M. Wang, X. Chen, X. Hou, Continuous water-water hydrogen bonding network across the rim of carbon nanotubes facilitating water transport for desalination, Nano Res. 14 (2021) 2171–2178, https://doi.org/10.1007/s12274-020-3173-2.

[116] G. Hummer, J.C. Rasaiah, J.P. Noworyta, Water conduction through the hydrophobic channel of a carbon nanotube, Nature 414 (2001) 188–190, https://doi.org/10.1038/35102535.

[117] X. Song, S. Li, W. Zhang, H. Liu, J. Jiang, C. Zhang, Constructing semi-oriented single-walled carbon nanotubes artificial water channels for realized efficient desalination of nanocomposite RO membranes, J. Membr. Sci. 663 (2022) 121029. https://doi.org/10.1016/j.memsci.2022.121029.

[118]A. Berezhkovskii, G. Hummer, Single-file transport of water molecules through a carbon nanotube, Phys. Rev. Lett. 89 (2002) 64503, https://doi.org/10.1103/PhysRevLett.89.064503.

[119]Kalra, S. Garde, G. Hummer, Osmotic water transport through carbon

nanotube membranes, Proc. Natl. Acad. Sci. 100 (2003) 10175–10180, https://doi.org/10.1073/pnas.1633354100.

[120]R.H. Tunuguntla, F.I. Allen, K. Kim, A. Belliveau, A. Noy, Ultrafast proton transport in sub-1-nm diameter carbon nanotube porins, Nat. Nanotechnol. 11 (2016) 639–644, https://doi.org/10.1038/nnano.2016.43.

[121]R.H. Tunuguntla, R.Y. Henley, Y.-C. Yao, T.A. Pham, M. Wanunu, A. Noy, Enhanced water permeability and tunable ion selectivity in subnanometer carbon nanotube porins, Science 357 (2017) 792–796, https://doi.org/10.1126/science.aan2438.

[122]Y. Li, Z. Li, F. Aydin, J. Quan, X. Chen, Y.-C. Yao, C. Zhan, Y. Chen, T. A. Pham, A. Noy, Water-ion permselectivity of narrow-diameter carbon nanotubes, Sci. Adv. 6 (2020) eaba9966, https://doi.org/10.1126/sciadv.aba9966.

[123]B. Liu, X. Li, B. Li, B. Xu, Y. Zhao, Carbon nanotube based artificial water channel protein: membrane perturbation and water transportation, Nano Lett. 9 (2009) 1386–1394, https://doi.org/10.1021/nl8030339.

[124] N. Naguib, H. Ye, Y. Gogotsi, A.G. Yazicioglu, C.M. Megaridis, M. Yoshimura, Observation of water confined in nanometer channels of closed carbon nanotubes, Nano Lett. 4 (2004) 2237–2243, https://doi.org/10.1021/nl0484907.

[125] Y. Zhang, C. Wang, C. Wang, Y. Zhang, J. Zhao, N. Wei, Lamellar water induced quantized interlayer spacing of nanochannels walls, Green Energy Environ. 9 (2024) 356-365. https://doi.org/10.1016/j.gee.2022.06.009.

[126] J. Shen, G. Liu, Y. Han, W. Jin, Artificial channels for confined mass transport at the sub-nanometre scale, Nature 6 (2021) 294-312, https://doi.org/10.1038/s41578-020-00268-7.

[127] H. Gao, J. Wang, X. Zhang, M. Hu, Q. Xu, Y. Xie, Y. Liu, R. Lu, Confined lamellar channels structured by multilayer graphene for high-efficiency desalination, Desalination 530 (2022) 115681, https://doi.org/10.1016/j.desal.2022.115681.

[128]X. Wen, T. Foller, X. Jin, T. Musso, P. Kumar, R. Joshi, Understanding water transport through graphene-based nanochannels via experimental control of slip length, Nat. Commun. 13 (2022) 5690, https://doi.org/10.1038/s41467-022-33456-w.

[129]W.-J. Zhao, L. Liang, Z. Kong, J.-W. Shen, A review on desalination by graphene-based biomimetic nanopore: From the computational modelling perspective, J. Mol. Liq. 342 (2021) 117582, https://doi.org/10.1016/j.molliq.2021.117582.

[130]A.T. Celebi, M. Barisik, A. Beskok, Surface charge-dependent transport of water in graphene nano-channels, Microfluid. Nanofluid. 22 (2018) 234505, https://doi.org/10.1007/s10404-017-2027-z.

[131]K. Guan, Di Zhao, M. Zhang, J. Shen, G. Zhou, G. Liu, W. Jin, 3D nanoporous crystals enabled 2D channels in graphene membrane with enhanced water purification performance, J. Membr. Sci. 542 (2017) 41–51, https://doi.org/10.1016/j.memsci.2017.07.055.

[132]K. Huang, G. Liu, J. Shen, Z. Chu, H. Zhou, X. Gu, W. Jin, N. Xu, High-efficiency water-transport channels using the synergistic effect of a hydrophilic polymer and graphene oxide laminates, Adv. Funct. Mater. 25
(2015) 5809–5815, https://doi.org/10.1002/adfm.201502205.

[133] W. Ma, T. Lu, W. Cao, R. Xiong, C. Huang, Bioinspired nanofibrous aerogel with vertically aligned channels for efficient water purification and salt-rejecting solar desalination, Adv. Funct. Mater. 33 (2023) 2214157. https://doi.org/10.1002/adfm.202214157.

[134] Y. Song, J. Phipps, C. Zhu, S. Ma, Porous materials for water purification, Angew. Chem. Int. Ed. 62 (2023) e202216724. https://doi.org/10.1002/anie.202216724.

[135] F. Li, G. Hanna, G. Yücesan, A. O. Yazaydin, Functionalization of metal−organic framework nanochannels for water transport and purification, ACS Appl. Nano Mater. 6 (2023) 3003−3011. https://doi.org/10.1021/acsanm.2c05389.

[136]Y.D. Yuan, J. Dong, J. Liu, D. Zhao, H. Wu, W. Zhou, H.X. Gan, Y.W. Tong, J. Jiang, D. Zhao, Porous organic cages as synthetic water channels, Nat. Commun. 11 (2020) 4927, https://doi.org/10.1038/s41467-020-18639-7.

[137] D. Hou, G. Qiao, P. Wang, Molecular dynamics study on water and ions transport mechanism in nanometer channel of 13X zeolite, Chem. Eng. J. 420 (2021) 129975, https://doi.org/10.1016/j.cej.2021.129975.

[138] J. S. Jang, Y. Lim, H. Shin, J. Kim, T. G. Yun, Bidirectional water-stream behavior on a multifunctional membrane for simultaneous energy generation and water purification, Adv. Mater. 35 (2023) 2209076, https://doi.org/10.1002/adma.202209076.

[139] Z. Yang, C. Wu, C. Y. Tang, Making waves: Why do we need ultra-permeable nanofiltration membranes for water treatment? Water Res. X 19 (2023) 100172. https://doi.org/10.1016/j.wroa.2023.100172.

[140] L. Ding, D. Xiao, Z. Lu, J. Deng, Y. Wei, J. Caro, H. Wang, Oppositely charged Ti3C2Tx MXene membranes with 2D nanofluidic channels for osmotic energy harvesting, Angew. Chem, Int. Ed. 132 (2020) 8720-8726. https://doi.org/10.1002/anie.201915993.

[141] D. V. Andreeva, M. Trushin, A. Nikitina, M. C. F. Costa, P. V. Cherepanov, M. Holwill, S. Chen, K. Yang, S. W. Chee, U. Mirsaidov, A. H. C. Neto, K. S. Novoselov, Two-dimensional adaptive membranes with programmable water and ionic channels, Nat. Nanotechnol. 16 (2021) 174-180. https://doi.org/10.1038/s41565-020-00795-y.

[142] Z. Qiu, J. Chen, J. Zeng, R. Dai, Z. Wang, A review on artificial water channels incorporated polyamide membranes for water purification: Transport mechanisms and performance, Water Res. 247 (2023) 120774. https://doi.org/10.1016/j.watres.2023.120774.

[143] M. D. Vincenzo, A. Tiraferri, V.-E. Musteata, S. Chisca, R. Sougrat, L.-B. Huang, S. P. Nunes, M. Barboiu, Biomimetic artificial water channel membranes for enhanced desalination, Nat. Nanotechnol. 16 (2021) 190–196. https://doi.org/10.1038/s41565-020-00796-x.

[144] M. D. Vincenzo, A. Tiraferri, V.-E. Musteata, S. Chisca, M. Deleanu, F. Ricceri, D. Cot, S. P. Nunes, M. Barboiu, Tunable membranes incorporating artificial water channels for high-performance brackish/low-salinity water reverse osmosis desalination, Proc. Natl. Acad. Sci. 118 (2021) e2022200118. https://doi.org/10.1073/pnas.202220011.

[145] S. Andreev, D. Reichman, G. Hummer, Effect of flexibility on hydrophobic behavior of nanotube water channels, J. Chem. Phys. 123 (2005) 194502, https://doi.org/10.1063/1.2104529.

[146] J.-Y. Li, Z.-X. Yang, H.-P. Fang, R.-H. Zhou, X.-W. Tang, Effect of the carbon-nanotube length on water permeability, Chin. Phys. Lett. 24 (2007) 2710–2713, https://cpl.iphy.ac.cn/Y2007/V24/I9/2710.